

**REPUBLIC OF TURKEY
ERCIYES UNIVERSITY
GRADUATE SCHOOL OF NATURAL AND APPLIED
SCIENCES DEPARTMENT OF MECHANICAL ENGINEERING**

**DESIGN AND AXPERIMENTAL INVESTIGATION OF THE
PAROBOLIC TROUGH SOLAR COLLECTOR**

**Prepared By
Ammar S. ALAMILI**

M. Sc. Thesis

**Supervisor
Assist. Prof. Dr. Yusuf TEKİN**

**May 2019
KAYSERİ**



**REPUBLIC OF TURKEY
ERCIYES UNIVERSITY
GRADUATE SCHOOL OF NATURAL AND APPLIED
SCIENCES DEPARTMENT OF MECHANICAL
ENGINEERING**

**DESIGN AND AXPERIMENTAL INVESTIGATION OF
THE PARABOLIC TROUGH SOLAR COLLECTOR**

(M. Sc. Thesis)

**Prepared By
Ammar S. ALAMILI**

**Supervisor
Assist. Prof. Dr. Yusuf TEKİN**

**May 2019
KAYSERİ**

COMPLIANCE WITH SCIENTIFIC ETHICS

I advertise that information in this study is acquired in accordance with ethical and academic rules. At the same time, I advertise that I transmit all materials and results that are not at the core of this work and I refer to them as required by these rules and behaviors.

Name-Surname: **Ammar S. ALAMILI**

Signature:



COMPLIANCE WITH GUIDELINES

"Design And Experimental Investigation Of The Parabolic Trough Solar Collector"
has been prepared accordance the Erciyes University Graduate Thesis proposal and
Thesis writing guidelines, and it was accepted as Erciyes University Graduate Thesis.



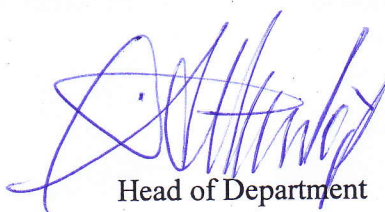
Owner of Thesis

Ammar S. ALAMILI



Supervisor

Associate Prof. Dr. Yusuf TEKIN



Head of Department

Prof. Dr. Necdet ALTUNTOP

ACCEPTANCE AND APPROVAL

The study titled “**Design And Experimental Investigation Of The Parabolic Trough Solar Collector** ”has been prepared by **Ammar S. ALAMILI** and has been supervised by **Associate Prof. Dr. Yusuf TEKİN** is accepted as the (M.Sc. thesis) in Erciyes University Graduate School of Natural and Applied Science / Department of Mechanical Engineering, by the jury.

07/05/2019

JURY:

President: **Doç. Dr. Mevlüt ARSLAN**

.....
.....

Member: **Prof. Dr. Veysel ÖZCEYHAN**

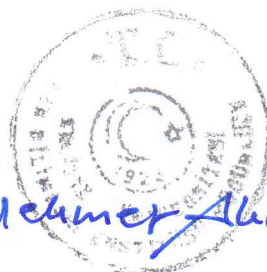
.....
.....

Member: **Dr. Öğr. Üy. Yusuf TEKİN**

.....
.....

According to decision dated 21.05.2019 and numbered 2019/31-02 acceptance of this thesis is approved by Graduate School Administrative Board.

...21.../05.../2019



.....
.....

Prof. Dr. Mehmet AKKURT

Director of the Institute

ACKNOWLEDGEMENTS

This thesis work is one of the projects presented to the Master of Science in Mechanical engineering program with emphasis on Structural Mechanics at, Erciyes University, graduate school of natural and applied sciences, mechanical engineering department. This work was carried out from the month of February 2018 to May 2019 at Erciyes University, Kayseri, Turkey.

I would like to introduce my great thanks and Gratitude to my supervisor, **Assist. Prof. Dr. Yusuf TEKİN** at Mechanical Engineering Department, Erciyes University, for his patient guidance, support and Encouragement throughout my entire work and for his valuable advice.

I would like to thanks my parents and my friends for all their love and encourage to me through my study. Also I would like to introduce all thanks and love to my wife who submit all the supports and helpful to me in this study and all time in my life. I would like to mention all the love and motivate in my life my lovely children (**Sara, Dima and Ayman**).

I dedicate this research

Kayseri, Turkey, May 2019

Ammar S. ALAMILI

**DESIGN AND EXPERIMENTAL
INVESTIGATION OF THE PARABOLIC TROUGH SOLAR COLLECTOR**

Ammar S. Ahmed ALAMILI

Erciyes University, graduate school of natural and applied sciences

MSc. Thesis, May 2019

MSc Thesis Supervisors: Assist. Prof. Dr. Yusuf TEKİN

ABSTRACT

The head line of this thesis is investigating in solar radiation as a main heat energy source. Through this research all the factors and properties that effect on heat energy gain were studied and investigated by use the parabolic trough collector.

This study is based on two aspects theoretical and experimental investigation. The theoretical part is covered by an excel program which includes all the equations and formulas that could calculate the entire requirement in this research. This research could classify in four main parts.

The first theoretical part of this research illustrates the solar radiation calculations which could compute the amount of beam solar radiation on the earth per meter square at any point on the earth in any time of the year.

The second part in this research shows the calculations of the amount heat solar energy that get from the parabolic trough collector, the collector efficiency, moreover the amount of steam that could get it from the collector.

The third theoretical part of this research illustrated the heat gain according to the experimental aspect of the study, which is representing the actual heat gain from collector.

The fourth part of the research is the experimental aspect. In this part a parabolic trough collector system is designed and manufactured to could calculate and estimate the actual heat efficiency of the system and compare it with theoretical aspect.

In the designed tube type solar collector, it was determined that the maximum energy theoretically is 880 W / collector and the experimentally is 835 W / Collector obtained in the hot water mode at noon on 09th of December, the collector efficiency was theoretically 63% and the experimentally 57%.

In the designed collector, the direct solar radiation measured on November 20 was 0.61 kg / h steam at 616 W / m^2 while the theoretical steam produce is 0.68 kg/h. The amount

could make by two-axis collector's solar tracking system is 1.107 Kg / h steam can be obtained.

Through the studying of this research some important points has found. There is a problem with winter season it make so difficult to rely on the solar energy without hybrid fuel station could offset the shortage in solar energy.

The other important point could illustrated the significant of the tilted collector to produce the maximum solar radiation if it could develop a new design of this collector could follow the sun in two directions to exploit the most fraction of the sun radiation.

Keywords: Solar radiation, Parabolic Trough Collector, Steam generation.



VAKUM TÜPLÜ PARABOLİK GÜNEŞ KOLLEKTÖRÜ TASARIMI VE DENEYSEL İNCELENMESİ

Ammar S. Ahmed ALAMILI

**Erciyes üniversitesi, Fen Bilimleri Enstitüsü Makina Mühendisliği Ana Bilim Dalı
MSc. Thesis, May 2019**

Tez Danışmanı: Dr. Öğrt. Üyesi Yusuf TEKİN

ÖZET

Bu çalışmanın amacı güneş enerjisinde daha etkin faydalanmak için parabolik oluk tipi güneş kollektörü tasarlamak ve enerji üretim performansını teorik ve deneysel olarak incelemektir. Teorik çalışmada, parabolik oluk tipi kollektöre gelen güneş enerjisinden elde edilebilecek faydalı enerjiyi hesaplamada Microsoft Excel programı kullanılmıştır. Çalışma dört bölümde tanımlanabilir. İlk kısımda dünyanın herhangi bir noktasında birim alana (m^2) düşen güneş ışınım miktarını hesaplanmıştır. İkinci kısımda, güneşi takip eden parabolik oluk kollektöründen elde edilebilecek güneş enerjisi miktarı, kollektör verimi ve buhar üretim miktarı teorik olarak hesaplanmaktadır.

Üçüncü kısmında ise, deneysel şartlarına göre güneşi takip eden parabolik oluk kollektörden elde edilen güneş enerjisi miktarı, kollektör verimi ve buhar üretim miktarı teorik olarak hesaplanmaktadır. Dördüncü bölüm ise tasarlanan parabolik oluk tipi güneş kollektörünün deneysel olarak incelenmesidir.

Tasarlanan oluk tipi güneş kollektöründe deneyin yapıldığı 09 Aralık öğle vakti için sıcak su modunda teorik olarak maksimum 880 W/kollektörenerji ve deneysel olarak 835 W/Kollektör enerji elde edildiği, Kollektör veriminin teorik olarak %63 ve deneysel olarak %57 olduğu belirlenmiştir.

Tasarlanan kollektörde 20 Kasım tarihinde ölçülen direk güneş ışınımı 616 W/m^2 de 0.61 kg/h buhar elde edilmiştir. Bu miktar kollektörün güneş takip sistemi iki eksenli yapılarak 1.107 Kg/h buhar elde edilebilir.

Tasarlanan parabolik güneş kollektörü hacim ısıtma amaçlı fosil yakıtlı sistemle bütünleşik kullanılması gerekmektedir. Enerji depolama sistemleri ile ısıtma süresi uzatılabilir. Ayrıca güneş takip sistemi iki eksenli yapılarak daha verimli hale getirilebilir.

Anahtar Kelimeler: Güneş enerjisi, Parabolik oluk tipi kollektör, Buhar Üretimi.

CONTENTS

COMPLIANCE WITH SCIENTIFIC ETHICS	ii
COMPLIANCE WITH GUIDELINES	iii
ACCEPTANCE AND APPROVAL	iv
ACKNOWLEDGEMENTS.....	v
ÖZET.....	vi
ABSTRACT.....	vii
CONTENTS.....	ix
ABBREVIATIONS AND SYMBOLS.....	xii
TABLE LIST	xvi
LIST OF FIGURES	xvii
INTRODUCTION	1
THESIS AIMS.....	2
IMPORTANCE	3

CHAPTER 1

LITERATURE REVIEW

1.1 Solar Radiation Introduction	7
1.2 Energy Emitted By the Sun.....	8
1.2.1 Solar Constant.....	9
1.3 Sun-Earth Astronomy.....	10
1.4 Sun-Earth Geometry – Time.....	12
1.4.1 Latitude ϕ	12
1.4.2 Longitude ‘L’	13
1.4.3 Declination Δ	13

1.4.4 Hour Angle (Ω)	14
1.4.5 Sun Altitude (A).....	15
1.4.6 Solar Azimuth(γ)	15
1.4.7 Incidence Angle (θ) On Sloped Plane (B)	16
1.4.8 Sunset, Sunrise & Day Length	17
1.4.9 Extraterrestrial Radiation	18
1.5 Direct, Diffuse and Reflected Radiation	19
1.5.1 Radiation Extinction Processes In The Atmosphere.....	19
1.5.2 Air Mass	21
1.5.3 Estimation of Clear-Sky Radiation.	22
1.6 Concentrated Solar Thermal Energy Introduction	24
1.7 What Is Concentrated Solar Power?.....	27
1.8 Distribution of the Solar Resource for Csp	28
1.9 Csp Energy Production Technologies	30
1.9.1 Parabolic Trough Collector Technology.....	30
1.9.2 Linear Fresnel Collector Technology	32
1.9.3 Solar Tower Technology.....	34
1.9.4 Stirling Dish Technology.	36
1.10 Storage Systems.....	37
1.10.1 Two-Tank Direct System:	38
1.10.2 Two-Tank Indirect System:.....	38
1.10.3 Single-Tank System:	39

CHAPTER 2

MATERIAL AND METHOD

2. Thermal Performance of Parabolic Trough Collector	41
2.1 Theoretical Thermal Performance of (Ptc)	41
2.1.1 Collector Geometrical Calculations	41
2.1.2 The Collector Heat Losses	49
2.1.4 The Collector Heat Gain and Theoretical Efficiency.....	51
2.1.5 The Collector Steam Generation.....	53

2.1.6 The Calculation by Excel Program.	54
2.2 Experimental thermal performance of (ptc).	59
2.2.1 Experimental Collector Manufacture and Install.	59
2.2.2 The Experiment Description.	60
2.2.3 The Experiment Efficiency.	66

CHAPTER 3

RESULT AND DISCUSS

3.1 Collector Theoretical Efficiency Result Analysis.....	68
3.1.1 Collector Efficiency with Aperture Dimensions.....	68
3.1.2 Collector Efficiency Change With receiver Tube Diameter.	70
3.1.3 Collector Efficiency Changes with Flow Rate.....	72
3.1.4 Collector Efficiency change with Receiver Tube Emittance.	74
3.1.4 Collector Efficiency and Indirect Properties.....	76
3.1.5 Calculation of Theoretical collector Efficiency.	76
3.2 Experimental Collector Efficiency.	86
3.2.1 Hot Water Experimental Efficiency.....	86
3.2.2 Steam Experimental Efficiency.....	101

CHAPTER 4

CONCLUSIONS AND RECOMMENDATIONS

4.1 Conclusion.....	104
4.2 Recommendations	105
REFERENCES.....	106
CURRICULUM VITAE.....	110

ABBREVIATIONS AND SYMBOLS

CSP	Concentrating Solar Power
CST	Concentrating Solar Thermal
SEGS	Solar Energy Generating System
E	Irradiance (power received per area w/m^2)
H	Energy received per area j/m^2
WH	Energy used watt- hour wh/m^2 .
t	Time
T	Solar constant
σ	Stefan- Boltzmann constant
T	Temperature
Am	Air mass
n	Number day of the year
ϕ	Latitude angle
L	Longitude
δ	Declination angle
ω	Hour angle
E	Equation adjustment time
L_{st}	Longitude standard meridian
L_{loc}	Real longitude of specific location
T	Solar constant
σ	Stefan- Boltzmann constant
T	Temperature
Am	Air mass
n	Number day of the year

ϕ	Latitude angle
ρ	Density
α	Sun altitude
γ	Solar azimuth
θ	Incidence angle.
β	Angle of tilted surface
ω_s	Angle sun set
H_o	Extraterrestrial radiation daily on surface
I_o	Extraterrestrial radiation hourly on surface
G_b	Beam radiation
G_d	Diffuse radiation
τ_b	Atmospheric transmittance for beam radiation
τ_d	Atmospheric for diffuse radiation ratio
htf	heat transfer fluid
PTC	parabolic trough collector
A_{ap}	Aperture area
f	Focal length
ψ	rim angle
A_r	Receiver area
ϵ_r	Receiver Emittance
ϵ_c	Cover Emittance
T_i	Fluid Temperature inside collector.
T_a	Ambient temp
hfi	Heat transfer coefficient inside the tube
k_p	Conductivity of pipe receiver

ρ	Reflectivity of the reflector.
\dot{m}	Mass flow rate k_i
c_p	Specific heat with constant pressure
A	Represent the altitude of the observer
U_L	Heat loss coefficient
Q_{loss}	Heat losses
D_r	Receiver diameter
D_c	Cover diameter
h_w	Wind heat transfer coefficient
L	Collector Length
T_{sky}	Sky temperature
Re	Renold number
ρ	Air density
V	Speed of wind
μ	Dynamic viscosity of air
k_a	Air thermal conductivity
N_u	Nusselt number
T_{CO}	Outside cover temperature
T_{ci}	Inside cover temperature
T_r	Receiver temperature
S	Energy reaches to the absorber tube receiver
α	Absorbance
τ	Transmittance of glass
F'	Collector efficiency factor
F_R	Collector heat removal factor
η_{th}	Theoretical thermal efficiency

η_{exp}	Experimental thermal efficiency
η_{steam}	Evaporator experimental efficiency
h_{fg}	Fluid gas water enthalpy



TABLE LIST

<i>Table 1. 1</i> Day number of the year.....	14
<i>Table 1. 2</i> Description of CSP technologies	26
<i>Table 2. 1</i> Show the collector and system parameters	45
<i>Table 3. 1</i> Experimental data table for hot water	98
<i>Table 3. 2</i> Experimental data table for steam.....	103



LIST OF FIGURES

<i>Figure 1. 1</i> Spectral distribution for wavelengths of radiation [3].	9
<i>Figure 1. 2</i> Relation between earth and sun by distance and diameter.[4].	10
<i>Figure 1. 3</i> Earth's orbit around the sun. [3][10].	11
<i>Figure 1. 4</i> Latitude angle with earth center	12
<i>Figure 1. 5</i> Latitude and longitude earth angles	12
<i>Figure 1. 6</i> Longitude angles with green which	13
<i>Figure 1. 7</i> Longitude and Latitude angles	13
<i>Figure 1. 8</i> Declination angles of earth.	14
<i>Figure 1. 9</i> Sun solar azimuth(γ) and altitude (α) angles.	16
<i>Figure 1. 10</i> Tilted surface angle (β)	17
<i>Figure 1. 11</i> Atmospheric processing extinction	20
<i>Figure 1. 12</i> Long of path in air mass changing with zenith angle.	22
<i>Figure 1. 13</i> The CSP plant parts and sub-systems.	25
<i>Figure 1. 14</i> CSP Types technology.	26
<i>Figure 1. 15</i> Resource of Solar for CSP technologies (DNI in kWh/m ² /y).	29
<i>Figure 1. 16</i> Viable Economic locations for CSP	30
<i>Figure 1. 17</i> PTC power plant.	32
<i>Figure 1. 18</i> Collectors Field of PTC plant.	32
<i>Figure 1. 19</i> LFCS power plan.	33
<i>Figure 1. 20</i> LFCS platform solar reflector.	33
<i>Figure 1. 21</i> Solar field of tower plant.	35
<i>Figure 1. 22</i> Solar field of tower plant.	35
<i>Figure 1. 23</i> Dishes/engines power plant.	37
<i>Figure 1. 24</i> Structure of dish from both sides.	37
<i>Figure 1. 25</i> Direct two-tank power plant.	38
<i>Figure 1. 26</i> Indirect (two-tank) storage system.	39
<i>Figure 1. 27</i> Single-tank storage system.	40
<i>Figure 2. 1</i> Path of reflected parallel rays in parabolic	42
<i>Figure 2. 2</i> Cross section parabolic collector profile.	43

<i>Figure 2. 3</i> Variation of parabolic curvature and focal distance for fixed aperture.....	44
Figure 2. 4 The beam radiation calculation.....	55
Figure 2. 5 Collector calculations heat gain, theoretical efficiency & amount steam. ...	56
Figure 2. 6 Experimental calculation (heat gain & experimental efficiency).....	56
Figure 2. 7 Show sun altitude angles (α) hourly per number of day per year.....	57
<i>Figure 2. 8</i> Data need to fill in for collector theoretically, experimentally and radiation.	58
<i>Figure 2. 9</i> Design the collector profile arrangements from steel structure.	60
<i>Figure 2. 10</i> The first stage of hot water rotated in the system.	60
Figure 2. 11 The second stage of producing steam in the system.....	61
Figure 2. 12 Collector turn to the east at the morning.	62
<i>Figure 2. 13</i> Collector turn to the west at the evening and program register temperatures.	63
Figure 2. 14 The reflected radiation focused on tube receiver.....	63
Figure 2. 15 Adjustment water pump.....	64
Figure 2. 16 Flow meter.....	64
Figure 2. 17 Thermo cable temperature reader.....	64
Figure 2. 18 Ambient temperature indicator.....	64
Figure 2. 19 Pressure gauge & thermo cable.....	64
Figure 2. 20 Instrument to measure radiation.....	64
Figure 2. 21 Collector driver motor.....	65
Figure 2. 22 Pipeing insulation.....	65
Figure 2. 23 Manufacturing collector system in Erciyes University.	65
Figure 2. 24 Installs the piping system.....	66
Figure 3. 1 Shows the change of heat gain with aperture sizes.....	69
Figure 3. 2 Shows the change of collector efficiency with aperture sizes.....	70
Figure 3. 3 Shows change of receiver diameter with collector efficiency & flow factor	71
Figure 3. 4 Shows the change of heat losses with receiver tube radius.....	71
Figure 3. 5 Shows the change of heat gain with flow rate.	73
Figure 3. 6 Shows the change of flow rate with efficiency & flow factor (F").....	73
Figure 3. 7 Shows the change receiver tube emittance with flow factor & efficiency. ...	74
Figure 3. 8 Shows the change of receiver tube emittance with collector heat losses	75

Figure 3. 9 Shows the change of receiver tube emittance & diameter size with efficiency 76

Figure 3. 10 Shows the heat gain theoretically & experimentally in the day. 99

Figure 3. 11 Shows the collector efficiency theoretically & experimentally in the day 100



INTRODUCTION

Solar energy is considered one of the most important renewable energy sources about the world, it is an inexhaustible energy because of its continued renewal long as the universe and it is a safe energy that cannot be monopolized or controlled, it is a clean environmentally friendly energy.

The concentrated solar thermal technologies create high-temperature, high-quality energy that can be used to drive a variety of engineering processes. Concentrated solar thermal (CST) is attractive because of free solar radiation and plentiful, but must beat the significant engineering challenges.

Concentrated solar thermal consists of a series of spread reflectors that transfer during the day to focus the sunlight on the solar receiver. CST techniques have various theories and arrangements, but the same principle of process: The solar concentrator focuses solar radiation on a solar thermal receiver that absorbs solar radiation and converts it into thermal power. Concentrated solar thermal is not a new thought. Stories from its application go back like ancient times. In the scientific society, folklore suggests that Archimedes led attempts to focus the sun on Roman ships using a lot of reflective surfaces. The first contemporary profitable application of concentrated of solar thermal was the construction of the trough system in Egypt, which was built in 1913 to generate hot steam to pay a pump for irrigation of semi-arid farming land.

The Solar Energy Generating System (SEGS), commissioned between 1984 and 1990 in the U.S., was the first employ of concentrating solar for power production. The SEGS project consists of nine part through power plants that have sum 354 MW power generation ability. The project marked the start of a rebirth of concern in CST technology. The whole atmosphere from the summit of the Earth's atmosphere to the concentrator, and between the concentrator and receiver, impact the quality of the solar radiation. The

nighttime and daylight hours sequence, clouds, and dust in the atmosphere reason interruptions in the solar radiation reach the receiver. Interruptions must be considered, but energy storage technologies can reduce their negative properties on concentrated solar thermal action.

Concentrated of solar power (CSP) is an essential function of CST technology. The word involves both CST plants that are employed to produce electricity and concentrated photovoltaic (CPV) power plants. This dissertations focuses on CST's application for power generation only [1].

And during the pursue of the implementation of power plants CSP diverse sorts parabolic trough system, linear Fresnel reflector system, power tower system, dish engine system note that 90% of these power plants take on the principle of parabola trough system, this points out that this sort of power plants is the most efficient in expressions of design, cost and performance [2], and this trend as one of the motives to pick the topic of this research in the study of this sort of solar concentrators.

THESIS AIMS

Through our study, we aim to achieve a number of goals that can be summarized as follows:

- Performance analysis for both the theoretical and the experimental aspect of the solar energy concentration process by use the parabolic trough solar collector and study the Different factors influence the amount of energy useful.
- Develop an excel program it could calculate a solar radiation on the earth at any region and any time on the year, more over it could calculate the heat gain by the collector and the collector efficiency in both theoretical and experimental aspect.
- Manufacture and tested a parabolic trough collector in ERCYES University to use it in study the actual performance and behavior for this type of solar concentrated technology.
- Use a parabolic trough collector to produces hot water and steam to simulator the real electrical power station and understanding the real factors that could affect directly on the collector performance.

IMPORTANCE

The concentrated solar power (CSP) uses renewable solar source to generate electricity at the same time the greenhouse-gases which it could produce is very low. Therefore, this technology has a strong chance to be the key method that decreases the climate change. Furthermore, the limited reservoirs of the traditional energy sources make it have a short life time period and that make this technology have a big chance to be alternative source of the traditional energy resources.

The concentrated solar power stations unlike the solar photovoltaic (PV) technology can produce electricity continually after the sunset or even when the cloud closes the sun because it could use the storage technology. The (CSP) technology could also supply other important demands like the heat energy for industry, the heating, and water desalination.

The recent studies show that generating steam power from solar energy is a new trend among the other energy sources researches. The large amount of solar energy is available that let to get a high level of steam energy which make it able to be the alternative energy required. The parabolic trough collector (PTC) which is the basic of our study considers the basic technology in this field to achieve this goal.

Since turkey lacks to traditional energy sources such as fossil fuels, it aims to exploit renewable energy, including the solar energy. Whoever, it is noted that this type of technology has not yet been used in this country. From other hand it is noted that Iraq and many other countries in the area which they have a high density of solar radiation but they still far away from this clean cheap technology. The importance of this study is to increase highlight the research on the solar energy technology in these countries to can matching with the progressing countries in this important field. This study can contribute by the theoretical and practical aspects as a reference to assessment of the efficiency of this type of technology as a source of alternative energy generation in turkey, Iraq and other countries in the area.

CHAPTER 1

LITERATURE REVIEW

To study in the field of solar concentrated solar radiation it is suitable to list a review of the theoretical and experimental work in this field for the 10 years ago and get the summarized results for their thesis. Some of the most relevant are presented below:

Rolim, M., Fraidenraich, N., 2009. An analytic prototype for a solar thermal electric produce system with parabolic trough collectors was improve. The energy diversion of Solar irradiation to thermal energy along the receiver tube of the parabolic collector is investigated, considered the heat losses non-linearity and its dependence on the local temperature. Three fields of different collectors were considered, the first field with evacuated absorbers, the second with non-evacuated absorbers and the third with bare absorbers. Finally, the output power of the plant is analyzed as a function of the evaporation temperature of the water-vapor fluid. A large maximum of the overall cycle efficiency is found for evaporation temperatures around 320 °C. Good agreement is obtained when comparing the results of this model with experimental data belonging to the Solar Electric Generating System [3].

Fernández, A., Zarzaa, E., 2010. The study shows an overview of the (PTC) which built and marketed through the last century, as long the prototypes presently under development. Also it presents a survey of systems which could incorporate this type of concentrating solar system to supply thermal energy up to 400 °C, especially steam power cycles for electricity generation, including examples of each application [4]. Liu, Q., Yang, M., 2012. Studying the sophisticated thermal physics mechanisms of the (PTSC) systems takes an energetic role in efficiently using the solar energy. Numerical simulations are done to assess the feasibility and efficiency where a data sample derived from the experiment and the simulation outcomes of two solar collector systems with 30

m² and 600 m² solar fields. Several main rules like the solar collector efficiency rises with the growth of the solar flux and the quantity of the heat transfer fluid, so it declines with the rise of the inlet temperature of the HTF, are obtained [5].

Zhifen, L., Yuang, G., 2013. A site test model has been developed to assess the (PTSC) thermal performance at dynamic circumstances depend on the equations of energy balance and a thermodynamics investigation. A major advantage of this method paralleled with steady-state exam models is this model contains the influence of the instance angle on the whole collector performance of an extended row of collectors, more the model could be used in site to (PTC) in real circumstances that follow up the sun just along one axis. Moreover, the dynamic model forecasts to the temperature outlet, the produce energy and thermal efficiency are in well agreement with measured outcomes on both cloudy and clearness days, which shows that this model could supply rapid, credible at site test [6].

Reddy, K.S., Kumar, K., 2015. A performance of (SPTC) with two traditional and four porous disc receivers is distinguished in constant time period, acceptance angle for the collector, highest performance, daily performance and heat loss exams. The exams are done for extensive range of flow rates (100 L/h–1000 L/h) and weather circumstances. Depend of experimental analysis, a constant time of a (PTC) is diverse from 70 s to 260 s for various absorber tube shapes. Heat losses from (PTC) are in the variety of 455 W/m²–1732 W/m² for average liquid temperature of $T_{\text{omb}} + 30\text{ }^{\circ}\text{C}$ [7].

Jebasingh, V.K., Joselin, G.M., 2016. This study focuses on the performance and efficiency of solar parabolic trough collector in India. It also reviews the pertinent applications of solar energy such as air heating system, desalination, refrigeration, industrial heating purposes and power plants. This paper will be useful for researchers concentrating on solar energy using parabolic trough collector [8].

Wanjun, Q., Wang, R., 2017. The research shows a promising methodology for effectiveness dropping the cosine loss for the scalable (PTC), supplying the probability of enhance a yearly average collector efficiency and achieving cost-efficient of using solar energy. A recent commercial (PTC) has a yearly average efficiency of nearly 50%, and the low efficiency range outcomes by the cosine loss. This study, a 300-kW_{th} (SPTC) with north south and flexible rotate axis follow up is primarily offered [9].

Hoseinzadeha, H., Kasaeian, A., 2018. The aim of this research is depend on a parabolic trough solar collector geometric analysis in diverse sizes of the major system's components. A range of Local Concentrated Ratio on an absorber tube and the visual

efficiency are two major advantage in geometric optimization of the (PTSC). The recent outcomes presented that the visual efficiency of 65% was got for the collector parts with the aperture width of 0.6 m, rim angle of 100° and absorber tube diameter of 0.025 m. Moreover, the visual efficiency of 61% was got with the aperture width of 0.7 m, rim angle of 90° , and diameter absorber tube of 0.025 m(3) [10]. Haojie, X., Yinshi, L., 2019. The active media (molten salt and artificial oil) take a blood role in transferring the solar energy to the solar power concentrated technic. Yet, transient characteristics for the artificial oil and molten salt are so less understood. It has shown that while molten salt which has high heat ability advantages, high thermal constancy and high process temperature has the ability to build the higher-efficiency CSP plant [11].

Hafez, A.Z., Attia, A.M., 2018. This study shows analyzing of deploying many parabolic trough solar collectors in a different countries and the study submitted and discussed operational SPTC plants too. A mathematical models let a different parameters calculation of parabolic solar trough system, the slop angle of the collecting surface and the acting of forces on the system. The experimental validate of the main mathematical models on practical parabolic solar trough concentrating. The paper shows the optical values of efficiency are close to 63% and the peak optical theoretical efficiency approached 75% [12]. Matteo, B., Simone, D., 2016. The study goals to analyzing absorber of a flat aluminum to heating process and generate steam directly in simpler linear focused solar collectors. It installed on an asymmetric concentrated parabolic trough to make a collector with a concentrating ratio of 42 that has investigated experimentally. Specially, a new test operation is submitted, applied and validate to describe the collector thermal performance through generated steam. The results show that a significant overall thermal efficiency of 64% can be made with negligible dropping pressure [13]. Karima, G., Safa, S., 2019. The thermal performance of (PTSPP) is critical to the total of the system efficiency. That sort of the solar power concentrated collector is investigated to the indirect of producing steam system. Some factors, as absorber thermal description; the mixed heating exchanger's efficiency; thermal efficiency, concentrated ratio and the quantity of steam producing. It found the efficiency of thermal energy fluctuates from 24% to 28% for PTSPP system so it approaches an average of concentrated factor near 200. The outcome that the steam generated extreme value by concentrated parabolic trough is 8 kg/h [14].

The head line of this thesis is investigating the theoretical and experimental behavior of the parabolic solar energy to produce the hot water and steam by fabricate a parabolic solar collector system in Kayseri city (turkey) and use excel program to calculate the theoretical and experimental results. In the designed tube type solar collector, it was determined that the maximum energy theoretically is 880 W / collector and the experimentally is 835 W / Collector obtained in the hot water mode at noon on 09th of December, the collector efficiency was theoretically 63 % and the experimentally 57%. In the designed collector, the direct solar radiation measured on November 20 was 0.61 kg / h steam at 616 W /m². While the theoretical steam produce is 0.68 kg/h. The amount could make by two-axis collector's solar tracking system is 1.107 Kg / h steam can be obtained.

From the above studies it could make a comparison between the results values of this study and the other previous studies results. The theoretical efficiency for both hot water & steam generation is 63% and the experimental efficiency was 0.57 for hot water and 61% for steam generation in this study while it could note that the thermal efficiency with Wanjun, Q., Wang, R., 2017 was nearly 50%, And with Hoseinzadeha, H., Kasaeian, result A., 2018 was 61% to 65%, And with Hafez, A.Z., Attia, A.M., 2018 the efficiency was 63% to 75% these results for hot water and for The steam generated efficiency with Matteo, B., Simone, D., 2016 was 64%, and with Karima, G., Safa, S., 2019. The thermal efficiency was 24% to 28% and it could note that for all electrical produce power system. The above researches show that the previous studies results are within our study range according to the specialist for varies studies factors and conditions.

1.1 Solar Radiation Introduction

The sun is the center of thermonuclear operations and generates a huge quantity of energy. The power released by the sun is called solar energy or solar radiation. In spite of the great distance between the sun and the earth, the amount of solar energy getting the earth is substantial. It is the earth's essentially natural source of energy and by a lengthy way.

The quantities of energy received at an appointed geographical site vary in time: between daylight and night because of the earth's turning around and between seasons due to the earth's tropic. And at a given time it also difference in space, due to the changes in the inclination of the solar radiation with longitude and latitude. Therefore, the quantity of energy received at a specified site and time rely on the relative site of the sun and the earth. This is why both sun-earth geometry and time perform a significant role in solar energy change and photo energy systems.

The quantity of solar radiation intercepted by the earth is called extraterrestrial radiation. As it makes its path towards the ground, it is exhausted when transit out of the atmosphere. On average, minimal than half of extraterrestrial rays get ground level. Even while the sky is so clear with no clouds, roughly 20 % to 30 % of extraterrestrial rays are lost through the downward pathway. A good knowing of the visual properties of the atmosphere is essentially to model the exhaustion of the radiation.

Role of the clouds is of essential value: visually thin clouds let a little amount of rays to arrive at the ground. Visually heavy clouds make darkness by halting the rays downwards. In clear sky, dust and water vapor are the major contributors to exhaustion [15].

1.2 Energy Emitted By the Sun

Any material emits electromagnetic radiation, on condition its temperature is over 0 K. The spectral irradiation is completely specified by temperature and the emitting characteristics of the surface of the material. The laws of Kirchhoff and Planck explain this operation. Solar radiation is nearly that of a blackbody (i.e., an ideal radioactive body) at a temperature of 5 780 K.

The emitted radiation extends through a very big spectrum, from X-rays to far infrared. However, nearly 99.9 % of the radiation emitted is existent among 0.2 μm and 8 μm and 98 % among 0.3 μm and 4 μm . Figure (1.1) shows the spectral allocation of extraterrestrial irradiation for the wavelength ranges [0.3, 1] μm and [0, 5] μm [15].

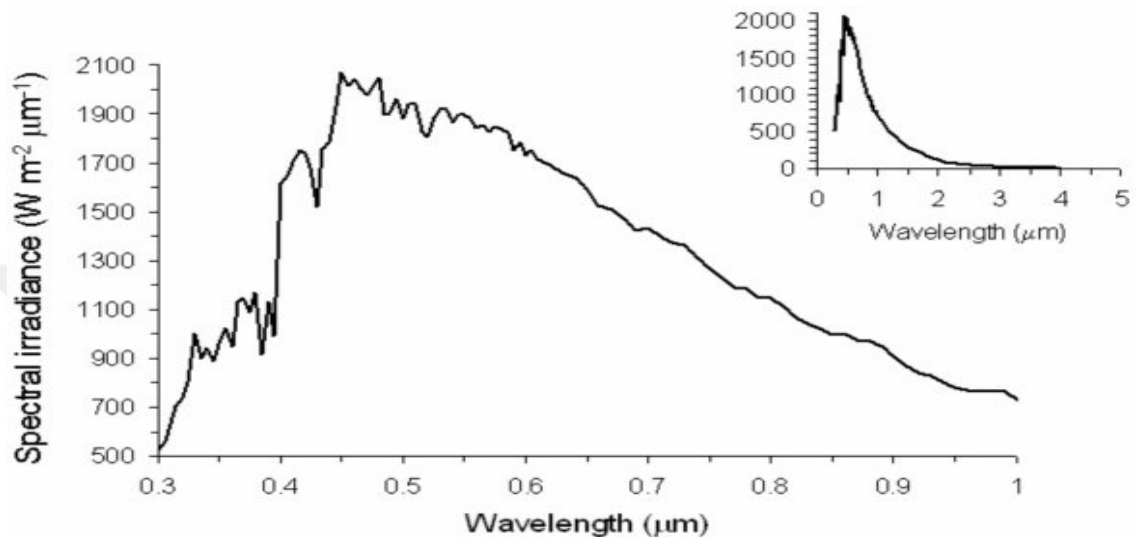


Figure 1. 1 Spectral distribution for wavelengths of radiation [15].

1.2.1 Solar Constant

Solar Constant is the density of the solar radiation hitting a square meter of the Earth or it is the density of radiation from the spherical black body, whose temperature is 57850K and diameter is 69610⁶ m, per square meter on a spherical surface whose radius is 150 10⁹m, and with the Sun located at its center [16].

$$G_{sc} = \sigma \cdot T^4 \cdot \left(\frac{4 \cdot \pi \cdot R}{4 \cdot \pi \cdot D}\right)^2 = 1367 \text{ w/m}^2 \quad (1.1)$$

Where

$\sigma = 5.67 \cdot 10^{-8} \text{ w/m}^2 \cdot \text{T}^4$ is the Stefan-Boltzmann constant.

$R = 696 \cdot 10^6 \text{ m}$ is the Sun radiuses.

$D = 1.496 \cdot 10^{11} \text{ m}$ is the average distance between the Sun and the earth.

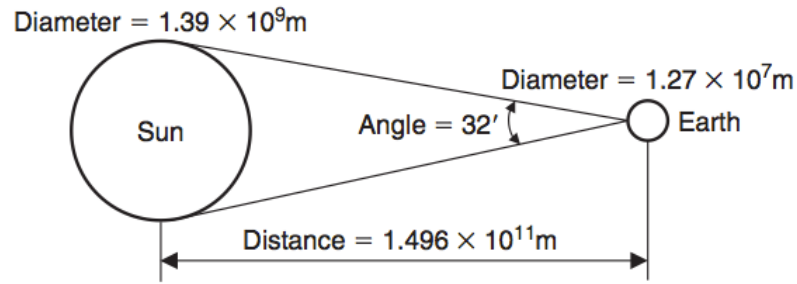


Figure 1. 2 Relation between earth and sun by distance and diameter. [16].

1.3 Sun-Earth Astronomy

The quantity of irradiation that arrive a specific spot at the upper of the atmosphere is ruled by the particular astronomical status of the earth on its orbit around the sun, its turning around its polar hub and the site of this spot on the earth.

The earth draws an elliptical orbit with the sun at one of the foci (Fig. 1.3). The eccentricity of the earth's orbit is so little (0.01675); this shows that the orbit is nearly circular. The average distance among the sun and the earth is about $150 \times 10^6 \text{ km}$. This distance is called 1 astronomical unit (ua). The Earth-Sun distance raises and reduces through year by near 1.7% in link to the average distance. As a result, the solar radiation on upper of the Earth's atmosphere is different by around 3.3% relative to the specific average value of 1367 w/m^2 . The solar radiation outside the atmosphere for a known day of the year (n) can be nearly in the following.

$$G_{on} = G_{sc} \left(1 + 0.033 \cos 360^\circ \frac{n}{365} \right) \quad (1.2)$$

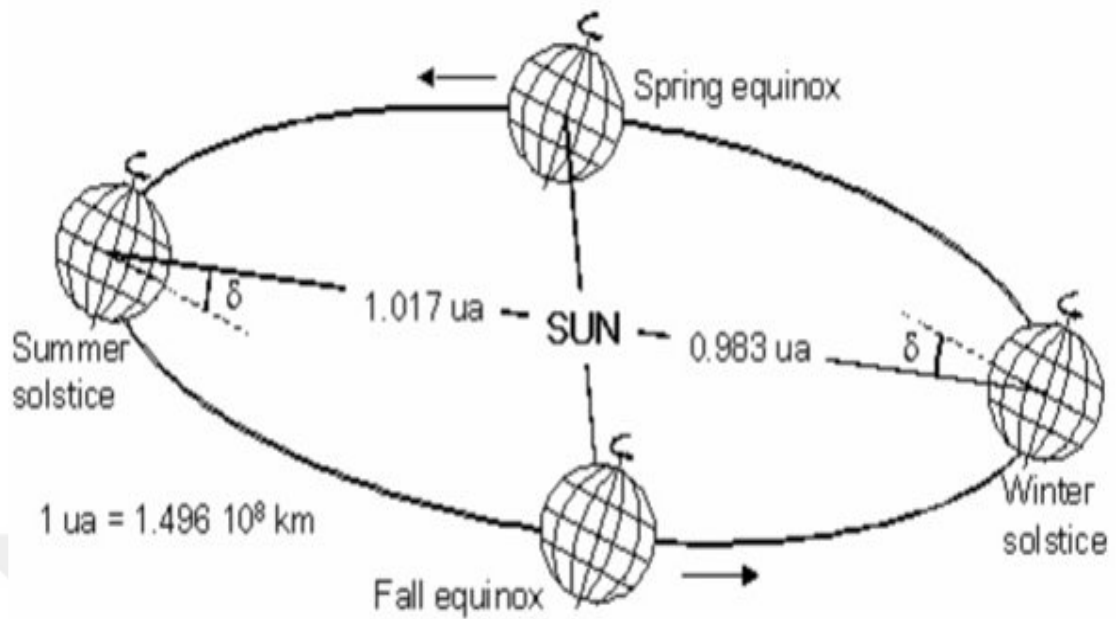


Figure 1. 3 Earth's orbit around the sun. [15][22]

In Figure 1.3, it can be observed that the equatorial level of the Earth tends at 23.45° at the level that contains the Earth's orbit. This is equal to say that the axis of daily turning round of the Earth transient from the poles is tilted in this angle relatively to the level of orbit. Due to this trend, the northern hemisphere is close up to the sun in July than the southern hemisphere.

On the contrary, the northern hemisphere is farther from the sun than the southern hemisphere through the astronomical winter that begins in December. Summer and winter weather are different in both hemispheres.

Finally, the daily turning round of the Earth itself leads to the thought of the average solar day divided into 24 hours of 60 minutes each. Parameters of time (year, day, hour) are necessary to calculate the apparent location of the sun in the sky, and therefore, radiation at the level of the earth that can be exploited [15] [18].

1.4 Sun-Earth Geometry – Time

The quantity of radiation reaching a certain spot in the upper part of the atmosphere is subject to the specific astronomical state of the Earth and its role around the Sun and its turning around the polar axis and the position of this spot on Earth. The whole solar radiation incident is calculated on an open surface after estimating time and solar location [15].

The various definitions below will be helpful in understanding the calculations of solar radiation:

1.4.1 Latitude ϕ

Latitude is used to show you near North or South to the equator. If you are on the equator then your latitude is zero. If you are near the North Pole or the South Pole, the latitude will be approximately 90 degrees.

Latitude is the measured angle in the center of the earth, among the level of the equator and where you are. Either north or south ranges from zero to 90 degrees [19].

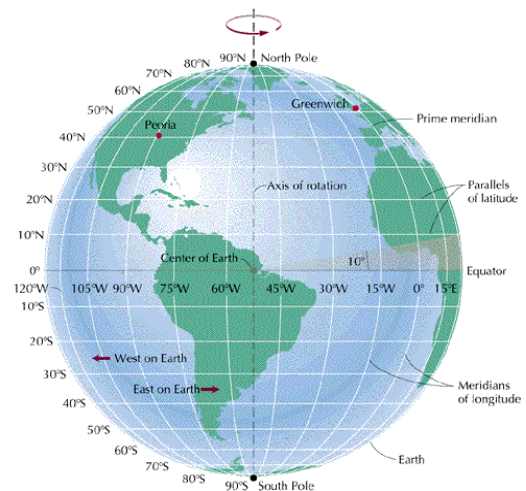


Figure 1. 4 Latitude angle with earth center

Figure 1. 5 Latitude and longitude earth angles

1.4.2 Longitude 'L'

Your longitude appears east or west for Greenwich. East Greenwich has longitude angles up to 180 degrees east. West Greenwich places have negative angles up to 180 degrees west. Longitude is the angle in the middle of the earth, between where you are and Greenwich. It Can be measured either east or west and range from 0 to 180 degrees [20] [21].

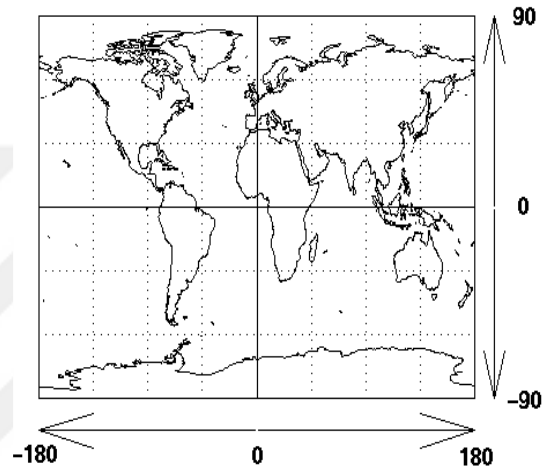
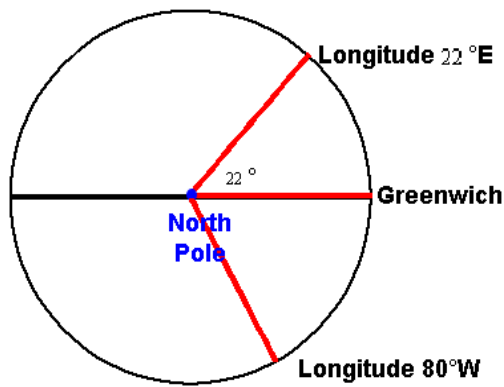


Figure 1. 6 Longitude angles with green which Figure 1. 7 Longitude and Latitude angles

1.4.3 Declination Δ

Decadence is the angle that arises among the level of the equator and the line that joins the center of the earth and the sun.

The deviation ranges from -23.45° to 23.45° which is positive through the summer and negative through the winter.

The deviation from the nearly equation can be found for Cooper [16].

$$\delta = 23.45 \cdot \sin \left(360 \cdot \frac{284 + n}{365} \right) \quad (1.3)$$

Where, n is the number of day in the year [17].

Table 1. 1 Day number of the year

Month	n for i:th Day of Month	For the Average Day of the Month		
		Date	n, Day of Year	δ , Declination
January	i	17	17	-20.9°
February	31 + i	16	47	-13.0°
March	59 + i	16	75	-2.4°
April	90 + i	15	105	9.4°
May	120 + i	15	135	18.8°
June	151 + i	11	162	23.1°
July	181 + i	17	198	21.2°
August	212 + i	16	228	13.5°
September	243 + i	15	258	2.2°
October	273 + i	15	288	-9.6°
November	304 + i	14	318	-18.9°
December	334 + i	10	344	-23.0°

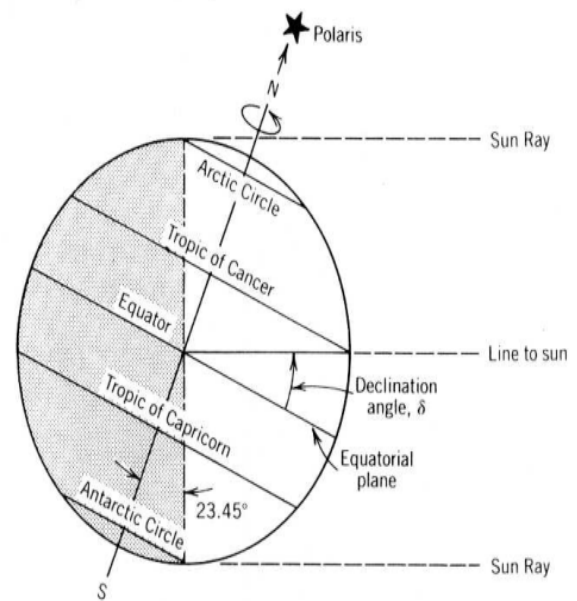


Figure 1. 8 Declination angles of earth

1.4.4 Hour Angle (Ω)

The hour angle is the sun's angular deviation from south

$$\omega = 15^\circ \cdot (\text{Solar time} - 12) \quad (1.4)$$

$180^\circ \leq \omega \leq 180^\circ$, negative before Solar Noon

Solar time is the time used in all sun angle relations; it does not match with the local time clock. It is needful to translate standard time to solar time by applying two modifications. Initial, there is a constant modification of the variation in the meridian between the path of the viewer (longitude) and the meridian on which the position standard is based. The sun needs 4 minutes to show 1° of the meridian.

The next modification is from the time equation, which needs into account disturbances in the earth's turning round rate that impact the time of the sun's passage of the observatory line. The variation in minutes between the time of the sun and the standard time is

$$\text{Solar time} = \text{standard time} + 4(L_{st} - L_{loc}) + E \quad (1.5)$$

where L_{st} is the standard meridian for the local time zone, L_{loc} is the longitude of the particular site, and longitudes are in degrees west, that is, $0^\circ < L < 360^\circ$. The factor E is the equation of time (in minutes) from Equation (1.6) [16].

$$E = 229.2 (0.000075 + 0.001868 \cos B - 0.032077 \sin B - 0.014615 \cos 2B - 0.04089 \sin 2B) \quad (1.6)$$

Where B is found from Equation (1.7) and n is the day of the year, Thus $1 \leq n \leq 365$.

$$B = (n-1) \cdot \frac{360}{365} \quad (1.7)$$

1.4.5 Sun Altitude (A)

The angle between the horizontal plane and the line joins the location with the center of the sun (the rise of the sun). [5].

$$\alpha = \sin^{-1}[(\cos \phi) \cdot \cos(\delta) \cdot \cos(\omega) + \sin(\phi) \cdot \sin(\delta)] \quad (1.8)$$

1.4.6 Solar Azimuth (γ)

The angle is integrated between the projections of the straight line at the location and the centers of the Sun at the horizontal and southern scales [16] [43].

$$\gamma = \sin^{-1} \left[\frac{\cos(\delta) \cdot \sin(\omega)}{\cos(\alpha)} \right] \quad (1.9)$$

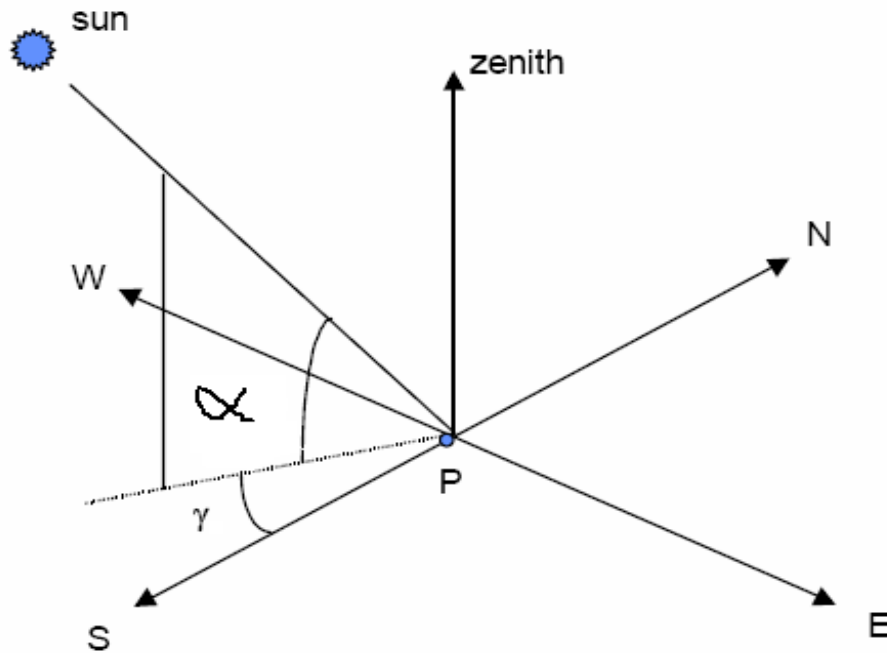


Figure 1. 9 Sun solar azimuth (γ) and altitude (α) angles

1.4.7 Incidence Angle (θ) On Sloped Plane (B)

Angle of sloping surface (β) is angle among the surface and the horizontal. Incidence angle on a surface of slope (β) and azimuth (γ) on the latitude (ϕ) at a time when the declination is (δ) and the hour angle is (ω), is:

$$\cos \theta = \sin \delta \cdot \sin \phi \cdot \cos \beta - \sin \delta \cdot \cos \phi \cdot \sin \beta \cdot \cos \gamma + \cos \delta \cdot \cos \phi \cdot \cos \beta \cdot \cos \omega + \cos \delta \cdot \sin \phi \cdot \sin \beta \cdot \cos \gamma \cdot \cos \omega + \cos \delta \cdot \sin \beta \cdot \sin \gamma \cdot \sin \omega \quad (1.10)$$

When the incidence angle (θ) of sunbeam falls on a horizontal surface it calls Zenith Angle (θ_z). It is found by inserting $\beta=0$ in incidence angle equation [33].

$$\cos \theta_z = \cos \phi \cdot \cos \delta \cdot \cos \omega + \sin \phi \cdot \sin \delta \quad (1.11)$$

$$0^\circ \leq \theta_z \leq 90^\circ$$

The incidence angle on surfaces with slope β due north or south at latitude ϕ is equal to the Zenith Angle at synthetic latitude ($\phi - \beta$) for the northern hemisphere, or ($\phi + \beta$) for the southern hemisphere[16].

$$\cos \theta_z = \cos(\phi - \beta) \cdot \cos \delta \cdot \cos \omega + \sin(\phi - \beta) \cdot \sin \delta \quad (1.12)$$

$$\cos \theta_z = \cos(\phi + \beta) \cdot \cos \delta \cdot \cos \omega + \sin(\phi + \beta) \cdot \sin \delta \quad (1.13)$$

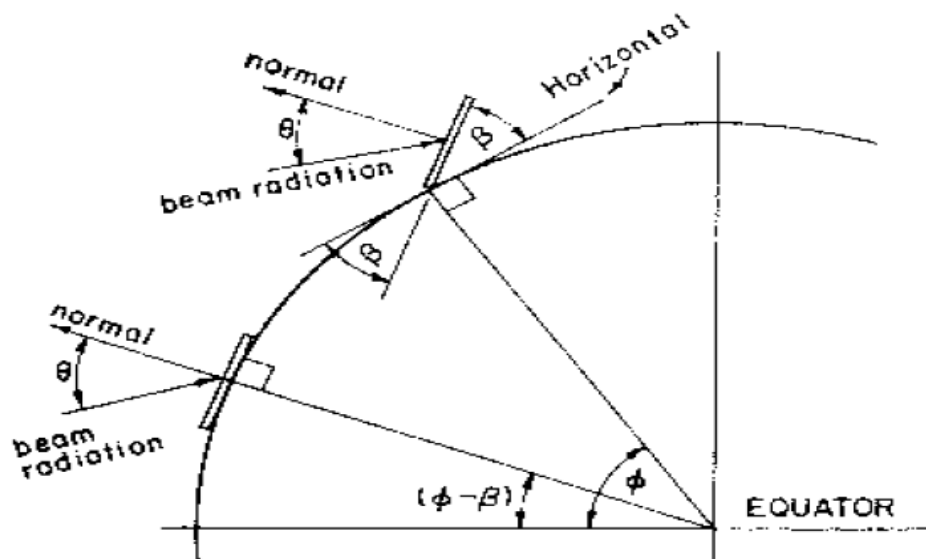


Figure 1.10 Tilted surface angle (β)

1.4.8 Sunset, Sunrise & Day Length

Equation (1.11) can be solved for the sunset hour angle ω_s , when $\theta_z = 90^\circ$:

$$\begin{aligned} \cos \theta_z &= \cos \phi \cdot \cos \delta \cdot \cos \omega + \sin \phi \cdot \sin \delta \\ \cos \omega_s &= -\tan \phi \cdot \tan \delta \end{aligned} \quad (1.14)$$

The sunset hour angle ω_s on surface with tilted towards the south

By (β) the equations be

$$\cos \omega_s = -\tan(\phi - \beta) \times \tan \delta \quad (1.15)$$

The sunrise hour angle is the negative of the sunset hour angle. as the hour angle increases $15^\circ/\text{hour}$, ω_s can be used to define the day length, it also follows that the number of daylight hours is given by[15][17].

$$N = \frac{2}{15} \cos^{-1} (-\tan \phi \cdot \tan \delta) \quad (1.16)$$

1.4.9 Extraterrestrial Radiation

Extraterrestrial radiation G_0 [W/m^2] is the radiation incident on the surface tangent to the outer surface of the atmosphere. It is function of zenith angle, θ_z , and refers to eq. (1.2) & eq. (1.11) we find the relation:

$$G_0 = G_{0n} \cdot \cos \theta_z. \quad (1.17)$$

$$G_0 = G_{sc} \cdot \left(1 + 0.033 \cos 360^\circ \frac{n}{365}\right) (\cos \phi \cdot \cos \delta \cdot \cos \omega + \sin \phi \cdot \sin \delta). \quad (1.17a)$$

It is a lot needful for calculation of daily solar radiation to have the integrated daily extraterrestrial radiation on a horizontal surface, H_0 this is gotten by integrating Equation (1.17a) over the time from sunrise to sunset. If G_{sc} is in watts per square meter ($G_{sc} = 1367 \text{ w}/\text{m}^2$). H_0 in daily joules per square meter per day is)

$$H_0 = \frac{24 \times 3600 G_{sc}}{\pi} \left(1 + 0.033 \cos \frac{360 n}{365}\right) \times \left(\cos \phi \cdot \cos \delta \cdot \sin \omega_s + \frac{\pi \omega_s}{180} \sin \phi \sin \delta\right) \quad (1.18)$$

Solar constant: G_{sc} [W/m^2], ($G_{sc} = 1367 \text{ w}/\text{m}^2$).

Daily radiation: H_0 [$\text{J}/\text{day} \cdot \text{m}^2$]

1.5 Direct, Diffuse and Reflected Radiation

Various extinctions conclude that not all radiation arriving the Earth's atmosphere reaching the Earth. In fact, as we shall see after that, just nearly 52% collide with the Earth's surface. In addition, dispersion raises the fact that part of the radiation reaching the Earth reaches diffuse radiation instead of straight radiation (or beam radiation). Diffused radiation has no favored direction.

Straight irradiation is the irradiation that reaches the Earth's surface in a directly line from the sun. Concentrated solar radiation systems can use beam radiation only. Non-directional irradiation cannot be focused and cannot be used in these systems.

Another part (including diffuse radiation) is involved in non-direct radiation. This part is not condemned to scattering, but to reflection on Earth: the reflected irradiation. It based on terrestrial reflectivity. As defined, it is different because it is much higher in refreshing snow compared to green grass.

Radiation on a surface in the atmosphere or on Earth is always the total of these three components: radiation from directed irradiation diffused irradiation and reflected irradiation. This amount is called total or global radiation.

Because concentrated solar power systems can use just direct irradiation, we will be more interested in direct radiation than diffuse and reflect radiation [18].

1.5.1 Radiation Extinction Processes in the Atmosphere

Some mitigation effects happen when radiation crosses the atmosphere. Commonly, they are called extinction. There are two common categories of extinction: absorption and dispersion (to be reflected a special case of scattering)

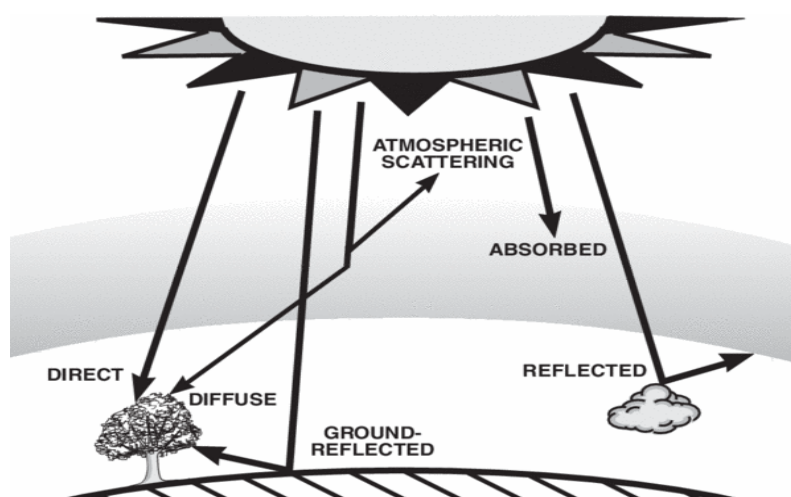


Figure 1. 11 Atmospheric processing extinction

The absorption known that the photon energy is processed by material. Scattering known as the radiation deviates from the direct diffusion.

Air absorption is an operation of extinguishing radiation that decreases the amount of solar radiation obtainable on the Earth's surface significantly. Some air components absorb radiation from a specific spectral range.

In the top layer of the atmosphere, O₃ absorbs nearly-short-wave radiation. The water vapor is strongly absorbed in the infrared friction of the solar spectrum, and carbon dioxide is another powerful infrared absorption agent. Because of gases, H₂O and CO₂, radiation move across the atmosphere is very low at wavelengths more than 2.5 micrometers. Lastly, oxygen and nitrogen absorb radiation above the large wavelength range.

Due to dispersion, solar radiation arrive the Earth's surface in part as diffused irradiation. Beam radiation is not the all radiation. Scattering does not change the radiation into other shape of energy. However, it decrease beam radiation.

Taking into account concentrated solar radiation systems, that use just beam radiation, scattering include a good radiation loss. In addition, coming radiation is partially propagated in space and does not reach the Earth's surface; therefore there is a real decrease in total radiation on the Earth's surface. Nearly one-fifth of whole radiation is reflected to the space. Clouds are the most important, as known, the most variable effects

on the total of solar radiation that arrive the Earth's surface are the result of these reflections, absorption and Scattering [18].

1.5.2 Air Mass

The effect of radioactive extinction on the atmosphere based on various sides such as dust concentricity, humidity and particularly clouds. These conditions are very changeful in a particular place and can just be specified by measurement. Another side, recognized without any measure, but only in geographical site and time: the pathway of beam solar radiation during the atmosphere.

Radiation attenuation bases on the last as follows: the longer path during the atmosphere is the greater radiation attenuation. The length of the path of solar radiation from the upper of the atmosphere to a specific site on the Earth's surface, contrariwise, would be a function of the geographical elevation of the site and the azimuth angle, z , the angle between the Earth's natural surface and the sun's line.

It could represent the relation as: If θ_z equals 0° , that is, if the sun is at the zenith, the ray directs must move to the minimum possible space within the earth's atmosphere till it arrives the surface. Conversely, if the sun is close to the horizon, the way during the atmosphere will be so long. Depend on that, it is possible to determine a relative measurement of the mass of air during which direct radiation crosses to the Earth's surface.

Light must pass during the lower mass of the atmosphere if the sun is at the zenith. This mass of the atmosphere gets the value of 1, if the site is considered at sea level. All other potential values must be linked to the least value. For instance, if the azimuth angle is 60° , the length of the path across the atmosphere is multiplied by 2. This value is called relative air mass or simply the air mass (AM).

The shape below illustrates the base of the Air Mass on the incidence angle of solar radiation[18].

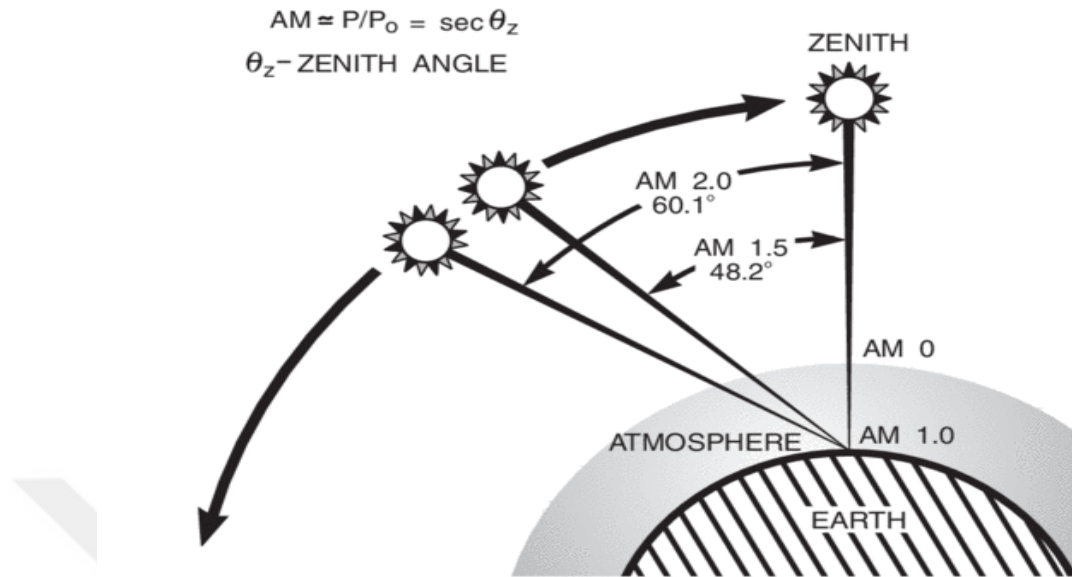


Figure 1. 12 Long of path in air mass changing with zenith angle.

1.5.3 Estimation of Clear-Sky Radiation.

The impacts of the atmosphere on dispersed and absorbent radiation change over time such as atmospheric conditions and atmospheric mass variable. It is valuable to describe the standard "clear" sky and the computation of the hourly and day radiation received on a horizontal surface over these standard conditions [16].

1.5.3.1 Beam Radiation

Atmospheric permeability in the beam is the proportion of direct radiation transmitted to the whole radiation incident at the upper part of the atmosphere. In (1976) it found a method represented for assessment beam radiation sent during a clear cover that takes into account the zenith angle and height of the standard envelope. Atmospheric transmittance of beam radiation τ_b is (G_b/G_0) and is given as follows:

$$\tau_b = \frac{G_b}{G_0} = a_0 + a_1 \exp\left(\frac{-K}{\cos \theta_z}\right) \quad (1.19)$$

The constants ($a_0 + a_1$), and K for the standard atmosphere which are given for high less than 2.5 km by

$$a_0 = 0.4237 - 0.00821(6 - A)^2 \quad (1.19. a)$$

$$a_1 = 0.5055 + 0.00595(6.5 - A)^2 \quad (1.19.b)$$

$$k = 0.2711 + 0.01858 (2.5 - A)^2 \quad (1.19.c)$$

(A)The altitude of the observer in kilometers. The clear-sky beam normal radiation is then Refer to Eq.1.17 the beam radiation can calculated as[16].

$$G_b = \tau_b \cdot G_{on} \cdot \cos \theta z. \quad (1.20)$$

$$G_d = 0.271 - 0.294 \cdot \tau_b \quad (1.20a)$$

1.5.3.2 Diffuse Radiation

Atmospheric permeability of diffuse radiation is the proportion of diffused radiation transferred to the whole radiation incident in the upper atmosphere. It is needful to assessment the radiation diffused in the clear sky on a horizontal surface to obtain the whole radiation. In (1960) it could developed an experimental relation between radiation transfer coefficients for beam and diffused radiation in clear days [16].

$$\tau_d = \frac{G_d}{G_0} = 0.271 - 0.294 \tau_b \quad (1.21)$$

$$G_d = \tau_d \cdot G_{on} \cdot \cos \theta z. \quad (1.22)$$

1.6 Concentrated Solar Thermal Energy Introduction

In 212 BC., it is said that Archimedes has used mirrors for the first time to concentrate the energy of the sun's rays. In 1615 it could invented a tiny solar powered engine which was a first registered machine application of solar energy. Its body component of glass lenses, a support structure and a metal container containing water and air.

A small water jet was produced when the air was heated and expanded through process. In the 1860s, it was suggested the thought of solar powered steam motor. In the next two decades, he with his assistant, construct the first solar powered motor and used it in a different applications. These engines have become the ancestors of modern parabolic collectors of solar focused applications.

These inventions established the basic of modern concentrated solar technology. With the drive to sustainable energy introduction and the growing awareness of the need to decrease carbon dioxide emissions, renewable energy resources have become an raise significant element in the global energy stability.

CSP systems have the possibility to take place the traditional fossil fuels. It will also help alleviate the potential impacts of climate change.

In CSP systems sunlight concentrated through visual devices. These concentrated rays produce heat that could be used either to produce vapor and electricity or to move chemical reactions. Nevertheless, since electricity is one of the major energy carriers in the world, electricity production is probable to be the primary application to become commercially applicable. Additional research and progress actions will play a key role in introducing this knowledge into the market [23].

Solar radiation, which reaches the Earth's surface, is a vital source of renewable energy. In a general view, solar radiation, which is consisted of photons, can be changed into electricity through photovoltaic or (CSP) systems.

This theory is focused just concentrated solar power techniques that use mirrors or visual lenses and focuses the sun ray to produce a high energy density and temperature grade.

These sorts of systems can just work with beam solar irradiation, so they are more likely to be used in regions where there are little clouds since other photovoltaic technology will fit better. The concentrated solar power component is four major subsystems, inclusive a focus system, a solar receiver, storage and / or additional fire (as a backup system) and a power block.

These subsystems are connected to each other by the transfer of fluid or radiation. The role of the solar receiver is to absorb focused solar energy and convert it to a heat transfer fluid (HTF).

The power block receives a rise temperature heat from the (HTF) and the storage tank storages solar heat coming from the transfer fluid. A scheme of the sub-systems of a concentrated solar plant as show in Figure (1.13).

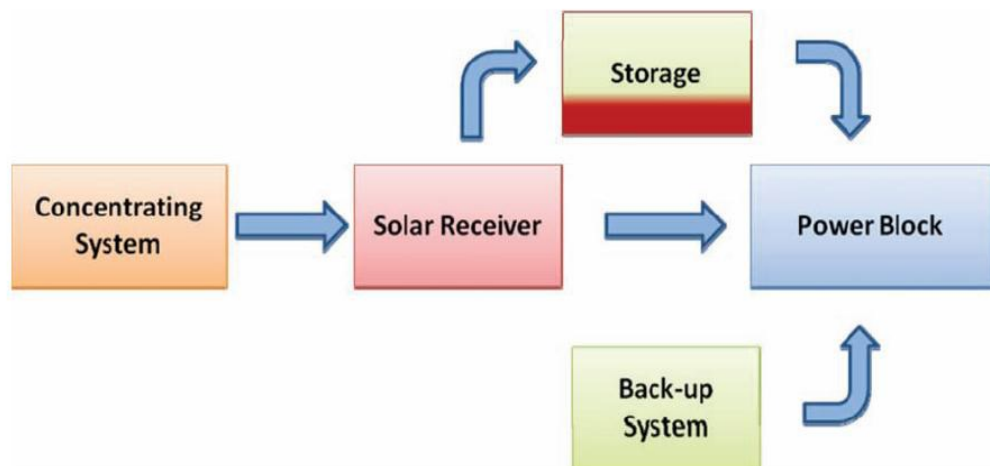


Figure 1. 13 The CSP plant parts and sub-systems.

Recently, there are four main families in concentrated solar power techniques, that could be classified by the method of concentrating sunlight and the technology used to receive solar energy.

Of the four current CSP techniques used to concentrate and collect sunlight to convert to heat, these CSP techniques are classified into two groups: those that concentrate on one-line sunlight and those that concentrate sunlight to a point, as shown in Fig. (1.14).

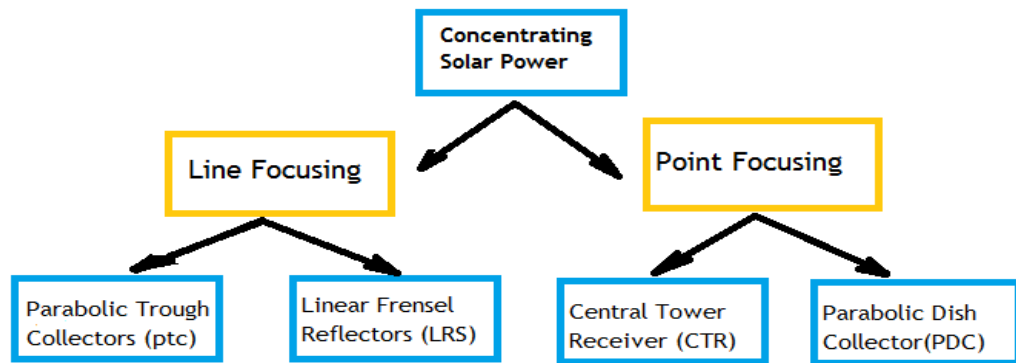


Figure 1. 14 CSP Types technology.

The main specifications of the four concentrated solar radiation technique shows in Figure 1.2 are characterize in Table 1.1, to better illustrate and highlight the main variation in processing temperature range for each technologies, present related costs, ripeness level, and concentration ratios [24].

Table 1.2 Description of CSP technologies

Technology	Working Temp. range(°C)	Focusing ratio	Ratio cost	Technology maturity
PTC	50-400	15-45	Low	Very mature
LFR	50-300	10-40	Very low	Mature
CTR	300-2000	150-1500	High	Most recent

1.7 What Is Concentrated Solar Power?

The classical virtual thesis predicts that the parallel ray beams with a spherical mirror axis will reflect the mirror and cross during the mirror sited at an $R / 2$ spaces from the mirror, where R is the mirror radius. The energy of the entire accidents captures light rays at this stage, with an effective focus of photovoltaic energy. This focus generates heat, thus the name: concentrated solar power energy. In short, CSP systems use various mirror / reflector arranged to convert the sun's energy into high-temperature heat. This heat could be used straight or changed into electricity. The main components of a CSP system are:

- **The Solar Collector Field:** These are a set of mirrors or reflectors that are collected the solar radiation and concentrated on the solar receiver. The fields are generally used in square meters which mean the surface area of the group, not the land use area.
- **The Solar Receiver:** The solar receiver is fraction of a system which converts solar radiation to heat. Occasionally this receiver is an integral fraction of solar collector area. The fluid of heat transfer, usually water or oil, is used in the solar receiver to transport the heat to the energy transformation system.
- **The Energy Conversion System:** The last component of the system changes heat into serviceable forms of energy, in the figure of electricity or heat.

The medium level of solar energy obtainable on the Earth's surface can be focused many times using CSP systems. The effectiveness with it this radiation can be changed into thermal energy based on a group of visual efficiency and heat conversion efficiency. The visual efficiency of the system is described by the accuracy of the reflective figure of the solar collectors. Thermal conversion efficiency is described by the physical properties of the solar receiver to change solar irradiation to thermal energy. Visual efficiencies up to 98% were accomplished with heat conversion efficiency between 70% and 95%.

In concentrated solar power systems that produce electricity, concentrated heat is used to generate vapor, either directly or indirectly that is then used to generate electricity. The

efficiency of this system, from solar to electricity, depends on the group of radiation, thermal efficiency and efficiency of the vapor cycle.

Concentrated solar power systems moreover could be used in chemical operations, for instance hydrogen or metal producer where concentrated solar radiation is used in direct way as heat resource [23].

1.8 Distribution of the Solar Resource for CSP

The major variations in direct sunlight obtainable from one site to another happen from atmospheric composing and weather. Direct normal insolation (DNI) is generally found in arid and semi-arid areas with clear and dependable skies, normally located at latitudes of 15 to 40 degrees north or south. Nearer to the equator, the weather is commonly so much cloudy and rainy in the summer, and at top latitudes the weather is so much cloudy. (DNI) is also much better at high altitudes, where the absorption and dispersion of sunlight is very lower.

Therefore, the main suitable areas for concentrated solar power sources are in North Africa, South Africa, the Middle East, Northwest India, the Southwestern United States, Mexico, Peru, Chile and the western part of China and Australia.

The Other regions may be convenient involve southern most of Europe and Turkey, and other sites in the southern United States, Central Asian countries, places in Brazil, Argentina, and other parts of China.

Current attempts to specify DNI source worldwide are depend on satellite information (Figure 1.15). Nevertheless, accurate measurements could just be accomplished through ground monitoring; satellite outcomes should as a result be measured with ground measurements to make certain accuracy [25].

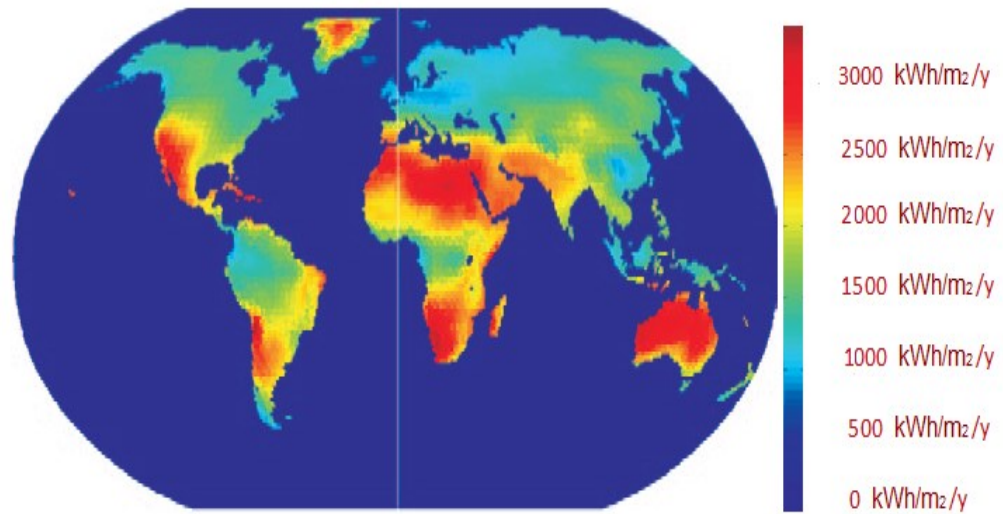


Figure 1. 15 Resource of Solar for CSP technologies (DNI in kWh/m²/y).

Unlike sister photovoltaic technique, concentrated solar heat needs a straight line of light to the sun to work at maximum efficiency. Global solar radiation involve of a range of direct and diffuse radiation. Solar thermal power plants can work only by beam radiation, whilst photovoltaic technique could use both direct and indirect radiation. The full use of CSP technology is limited to geographical location where yearly beam radiation levels are rise; the so-called solar belt area, where the yearly horizontal radiation levels range among 1800 kWh / m² and 2500 kWh / m² (Figure 1.16) [23].



Figure 1. 16 Viable Economic locations for CSP

Although "sun belts" on the ground are comparatively tight, the technological possible of CSP is enormous. If completely developed for CSP applications, the possible in the US Southwestern states will match the electricity supplies of the whole United States many times. The Middle East and North Africa possible will cover up around 100 times the present consumption in the Middle East and North Africa and the European Union joint. Shortly, the CSP will be mainly able to generate sufficient carbon, electricity or low-carbon fuels to match global request. Nevertheless, the main challenge is that request for electricity is not all time near the best energy collaboration program sources [25].

1.9 CSP Energy Production Technologies

Currently, there are four main CSP technology families, that could be classified by the method they concentrate the sun's rays and the technique used to receive the sun's energy [25].

1.9.1 Parabolic Trough Collector Technology

PTC collectors contend of solar collectors (mirrors), heat receivers and support structures. Mirrors are formed in an equal shape by forming a reflective sheet of reflective substance

into parabolic form that focuses the incoming sunlight on a central receiving tube in the focal line of the collector.

Mirrors arrays can be 100 meters (m) long or longer, with a curved aperture of 5 m to 6 m. A single axis tracking mechanism is used to direct together solar collectors and heat receivers towards the sun. This system is commonly installed align north-south and follows the sun as it transfer from east to west to make the most of energy collection.

The receiver consists of the absorption tube (usually metals) inside an evacuated glass cover. The absorption tube is usually a coated stainless steel tube, with a spectral selective layer that absorbs the solar radiation well, but emits so little radiation. This assists to decrease heat losses. Glass evacuate tube is used as it assists to decrease heat losses.

The heat transfer fluid is transported through absorption tubes to accumulate solar energy and convert it to the vapor generator or to the heat storage system, if exist. Greatly of the existing parabolic troughs uses artificial oils as (HTF), which is fixed up to 400 ° C. New plants are used under the exhibition of molten salt at 540 ° C either for heat convey and / or as middle for thermal storage. High-temperature molten salt may significantly proof thermal storage action.

Parabolic trough is the most mature of the CSP technologies and represent the frame of the present commercial plants [23].

In this system, the tube receiver is placed along the focal line of all reflectors in all parabola reflector form. The tube is installed on the mirror structure and the heat transfer fluid flows through and outside the solar mirrors field to where it is used to generate the vapor (or, in the case of the water / steam receiver, it is sent directly to the turbine) (Figure 1.17, 1.18).

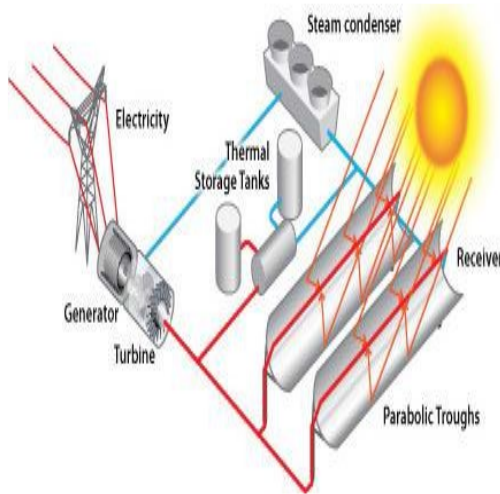


Figure 1. 17 PTC power plant.



Figure 1. 18 Collectors Field of PTC plant.

1.9.2 Linear Fresnel Collector Technology

Linear Fresnel collector (LFCs) is similar to parabolic trough collectors, but use a series of long flat or little bend mirrors arranged at various angles to focus sunlight on two sides of a constant receiver (install on some meters over the mirror field). Any line of mirrors is supplied with a left unidirectional tracking system and is improved individually to insure that the sunlight is continuing focused on the receivers. The receiver is provided with a long selectively-coated absorber tube.

Unlike the collectors of trough parabolic, the Fresnel collector's focal line is distorted by astigmatism. This needs a mirror over the tube (secondary reflector) to relocate rays that loss the tube, or many parallel tubes form a multi-tube receiver wide enough to get most of the concentrated sunlight with no secondary reflector.

The important advantages of linear Fresnel CSP systems compared to parabolic trough systems are that:

- LFCs are able to apply cheaper flat glass mirrors that are a standard product usually.
- LFCs need fewer steel and concrete, since the metal support frame is lighter.
- Wind forces on LFCs are minimal, out coming in better frame static, decreased visual losses and less mirror-glass damaged.

- Mirror surface for one receiver is higher in LFCs than in PTCs, so that is important, and it makes the receiver is the most expensive component in both PTC and in LFCs.

These advantages must be balanced with the fact that the visual efficiency of the LFC solar fields (in reference to direct solar irradiation on the cumulate mirror aperture) is less than the PTC solar fields because of the LFCs' engineering properties. The trouble is that the receiver is constant and when the time is morning or afternoon the efficiency of PTC is higher than LFC.

In spite of these holdbacks, the relative simplicity of the LFC system makes it perhaps cheaper to produce and install than PTC CSP plants.

Nevertheless, it stays to be seen if costs per kWh are chipper. moreover, given that LFCs are usually suggested to use direct steam production, addition thermal energy storage seems to be high expensive (Fig 1.19, 1.20) [23].

The challenging of design a cost efficient collector system is to warranty the demand of visual and mechanical quality of the subsystems like primary mirrors, tracking system and secondary reflector is cheapest. These quality sides have to be concerned not just through design stage but also through building on site[26].

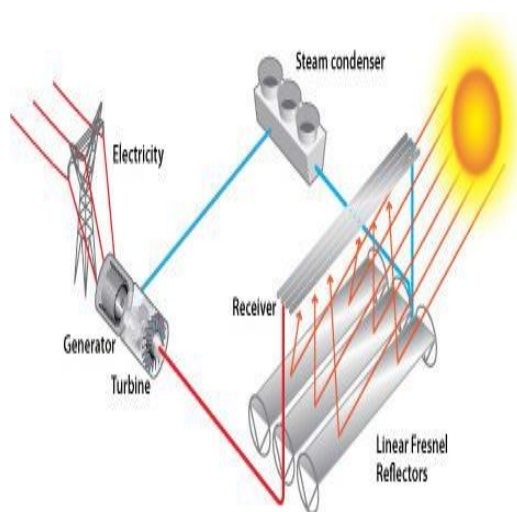


Figure 1. 19 LFCS power plan.



Figure 1. 20 LFCS platform solar reflector.

1.9.3 Solar Tower Technology

Solar tower techniques use a range of ground mirrors to concentrate the direct solar radiation on a high receiver installed on a central tower where the light is collected and changed to heat. The heat leads to a thermodynamic cycle, and in most states a water vapor cycle, to produce electricity. Solar field has contained a large number of mirrors that are controlled by the computer, known as heliostats which track the sun automatically in two axes.

These mirrors reflect sunlight on the central receiver at the area of the liquid heated. Solar tower could make temperatures higher than the PTC and linear LFC systems. Since extra sunlight be able to focus on one receiver, thermal losses can be reduced at this point.

Present solar towers use molten salt or water / steam to transfer heat to the heat exchanger, steam turbine system. based on the design of receiver and processing liquid, the maximum working temperatures be able to range from 250 ° C to 1000 ° C most likely for future plants, even if temperatures about 600 ° C will be standard with present designs of molten salt.

The normal size of today's solar tower technology plants domain from 10 MW to 50 MW and the size of the solar field in demand increases with desired of yearly electricity production, that leading to greater space between the receiver and the external mirrors of the solar field. This out coming in increased visual losses because of atmospheric absorption, inescapable angular mirror deflection caused by imperfections in mirrors and minor errors in mirror tracking.

Solar towers are able to use artificial oils or molten salt for heat transfer liquid and a storage middle as well to stockpile heat energy. Artificial oils restrict the working temperature to nearly 390 ° C that leads to restrict the efficiency of the steam cycle. It could increase the possibility of working temperature by use a molten salt to range between 550 and 650 ° C, which are sufficient to let higher efficiency supercritical steam cycles, even if the highly cost for these steam turbines perhaps a restriction. Instead of that it can use the direct steam generation (DSG), which is abolished the requirement and cost of heat transfer liquid, however this technique is at the early step of development and storage notion to use with the DSG yet require to be verified and avoided.

Solar tower has many advantages that perhaps make it become the favorite CSP technology. These advantages are:

- Higher temperatures may be permit higher efficiency in steam cycle and decrease water use to cool the condenser.
- Higher temperatures make using heat storage energy better to fulfill a schedulable power production.
- Higher temperatures let more temperature variance in a storage system, decrease costs or permitting higher storage to the equal cost.

The main advantage is the chance of using thermal energy storage to increase power factors and let an elastic generation strategy to increase the amount of electricity produce, furthermore fulfill higher efficiency grades. referring to that and other benefits, if could decrease the costs and operating expertise earned, solar tower most probably to fulfill a big ratio of the mart for the future, although PTC systems have dominate the mart yet. Solar tower technology still under demonstration, but in the long run it could supply less cost electricity than trough and dish systems (Figure 1.21, 1.22) [23].

The choice of heliostat material is an important side for designing a power plant. The huge mirrors represent nearly 50% from the whole system costs, and should be highly reflective and high performance, lightweight, simple to clean and anti-erosion. Many ways suggest to cleaning heliostat like use of pressurized air / water pressure according to different environmental situations [27].

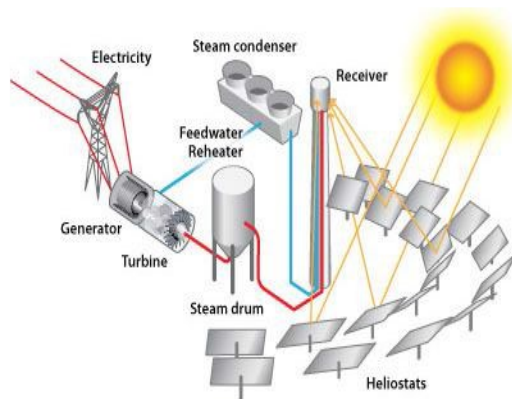


Figure 1. 21 Solar field of tower plant.



Figure 1. 22 Solar field of tower plant.

1.9.4 Stirling Dish Technology.

Parabolic dish–stirling system is the one of the CSP technology which has evolved for applications that let to get high temperatures focusing the radiation in a concentrate (P DS) system follows the sun and concentrate solar energy in the cavity receiver, so the receiver absorbs the energy and convey it to a heat engine/generator that produces electricity[30].

This system includes of a parabolic dish form focusing (as a satellite dish) which reflects beam solar radiation to a receiver at a dish focus. Receiver perhaps is a Stirling engine or a micro- turbine. Stirling systems need sun to be followed in two axes; however a high energy focus on a one dot be able to get great temperatures.

Most study now concentrates of using Stirling engine joint with generator part, placed in center of the dish, to change thermal energy to electrical energy. Recently two sorts of Stirling engines are used: Kinematic and Piston Free. Hydrogen used with kinematic engine as a liquid of working and it has upper efficiency than free piston. Helium used with Piston free without make friction through working, therefore needing maintenance is less.

Most important advantages of Stirling dish technique are the following:

- Position of generator - in general, to any dish in the receiver – works to decrease the losses of heat, that leads to the particular ability of dish-generating is little, highly modular (usual sizes between 5 to 50 kW) and are appropriate to allocation generation.
- Stirling dish technology is able to doing extreme efficiency among the kinds of CSP system.
- Stirling dish works with small and dry cooling system or cooling tower lets CSP to supply electrical power in arid regions.
- A "Stirling" dish can be placed, due to the fact that it is stand-alone, on slopes or terrain, unlike the solar tower, PTC and LFC.

The above advantages leads to Stirling dish technologies can match a high economically value several areas, despite a low cost of electrical power, it seems to be higher than other

CSP technologies. One aspect is the costs; other is the challenge of this technology is the difficulty of use storage. Stirling dish remains in the early stage and the product cost still uncertain. Because of its small size and high ability to extend , stirling can be the other option to solar photovoltaic in dry locations (Fig 1.243, 1.24) [23].

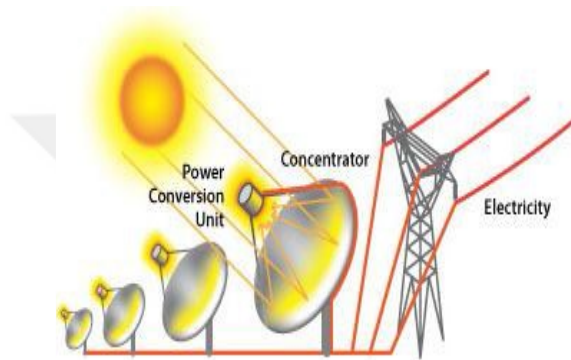


Figure 1. 23 Dishes/engines power plant



Figure 1. 24 Structure of dish from both sides.

1.10 Storage Systems

The main idea of using thermal energy storage is to expand the hours of electrical production in CSP plant. The solar field of The CSP plant is bigger than is demanded to let the steam turbine works with maximum capacity. The surplus heat produced through a shining hours in a day is transmitting to storage that able to be used then in the day to match the request of electric power what time sunset.

According to how large the solar field is compared to the turbine capacity, the thermal storage capacity able to expand working time of the CSP plant some hours when sun shutdown to 24 hours, running the base load [29].

The integration of thermal storage systems in CSP plants enables improved energy system efficiency, amendment of variation between active generation and the demand, enhanced energy discharge by this kind of plant, so simpler integration of electric power net [24].

Many thermal energy storage techniques are examined and executed which have involved: a direct two-tank system and an indirect system for two tanks and the system of cline thermo single-tank.

1.10.1 Two-Tank Direct System:

Solar thermal energy is stored by these systems in the same liquid operating to collect it. Liquid uses d in two tanks – the first in low temperature and second in high temperature. Liquid moves from low-temperature tank during solar collectors which are heated to maximum temperature before returns back to high storage tank. Liquid moves from a high temperature tank into a heat exchanger, when produce the steam to generate the electrical power. The fluid leaves heat exchanger in low temperature then come back in low temperature tank as shown in (Figure 1.25).



Figure 1. 25 Direct two-tank power plant.

1.10.2 Two-Tank Indirect System:

This system works similarly manner like the two direct systems of the tank, excluding for the use of various liquids like heat transfer liquid and storage. Utilization of these systems is just in plant which liquid of heat transfer is high cost or unsuitable to work with storage liquid.

Storage liquid runs from low temperature tank into an additional heat exchanger, heated with high temperature of the heat transfer liquid.

The heated liquid then runs back to storage tank at high temperature. The liquid leaves heat exchanger in low temperature then comes back to solar collector field to reheat again to high temperature. Storage liquid starts from the high temperature tank to produce steam in similar way as the direct two tanks system. An additional heat exchanger is needed in the indirect system and that lead to extra cost to the plant. This system normally used oil for heat transfer liquid and molten salt in storage tank as (Figure 1.26).

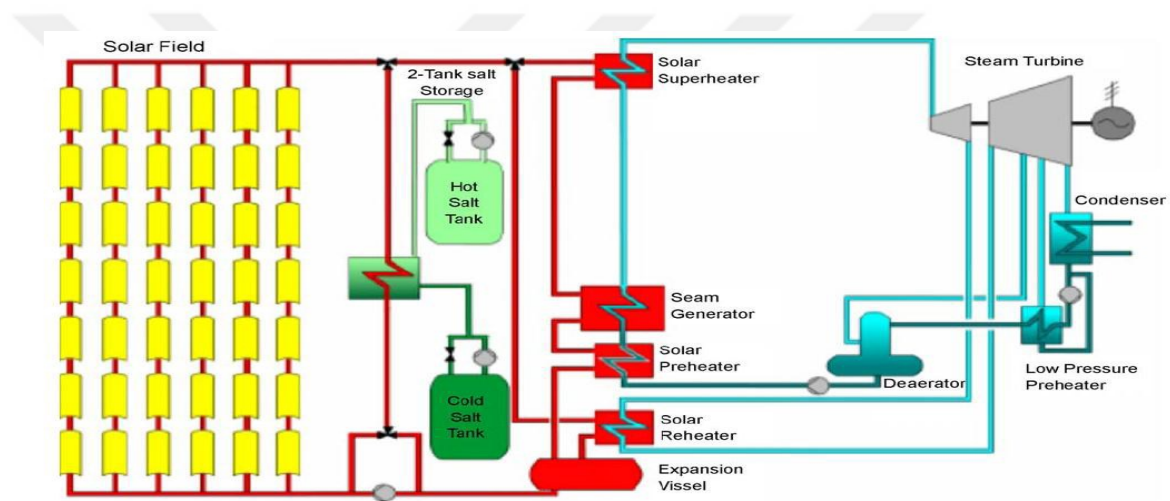


Figure 1. 26 Indirect (two-tank) storage system.

1.10.3 Single-Tank System:

Thermal energy is stored in this system by a solid middle – usually silica sand - found at the single tank. In every time through working, part of the middle is on high temperature while the other part of it is on low temp., Hot and cold temperature zones are detached with temperature slope. Heat transfer liquid which is heated in high temperature influxes in upper thermal layer and leaves from floor in low temp., this operation shifts thermal slope down so increases thermal energy for the system to storage. The flow inversion changes thermal chromatography upper so take off thermal energy from the system to produce steam and electrical energy.

The solid storage middle with one tank let this system cheaper than the other two tank systems (Figure 1.27) [30] [24].

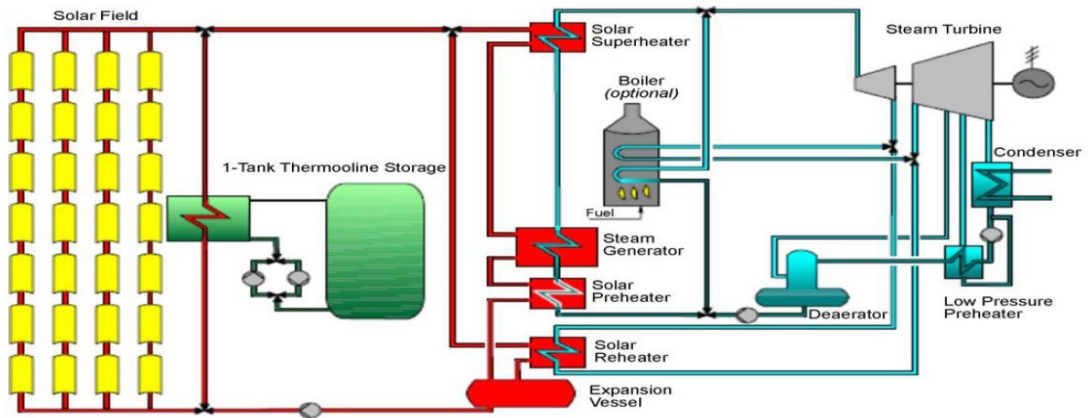


Figure 1. 27 Single-tank storage system.

CHAPTER 2

MATERIAL AND METHOD

2. Thermal Performance of Parabolic Trough Collector

In order to understand the performance and efficiency of collectors, we need to study some of the parameters and formulas of the theoretical and experimental sides and analyze their relationship and compare the results obtained from both sides to find the appropriate design and obtain more information about the appropriate conditions that must be met for high efficiency of the collector Somewhere.

2.1 Theoretical Thermal Performance of (PTC)

In this section, the thermal performance of PTC is studied with some parameters and formulas, then the results will be analyzed to understand the efficiency of the collector's performance in theory.

2.1.1 Collector Geometrical Calculations

The collector parabolic trough is curve has a cross-section figure like a part of parabola. For high accuracy, it is a similar section of a parabola about its top head. And it has focal line that contains focal points of parabolic sections. The beams Radiation which come in the plane parallel to the visual plane are reflected to the path which it passes during the focal line as shown in figure (2-1).

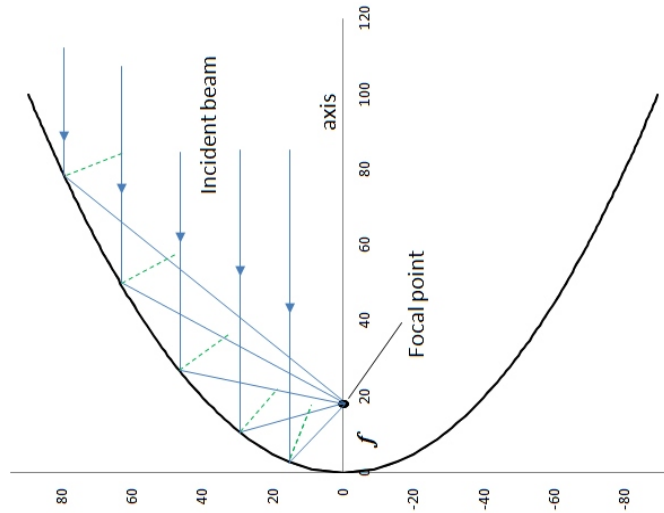


Figure 2. 1 Path of reflected parallel rays in parabolic.

To can describe a geometrically parabolic trough, the parabola should be specified, parabola cross section with several variables worked to recognize the form and volume of the parabolic trough must be specified: trough length, focal length, aperture width and rim angle.

The first step to design the collector is to select the dimensions of the collector which represent the aperture dimensions (width and length) [31].

The aperture is the opening from it solar radiation enters the concentrator. The aperture area A_{ap} is calculated as the product of the aperture width w and the collector length l :

$$A_{ap} = w \cdot l$$

There is an important cause to choose a parabolic concentrator. Because of the long distance from the sun the rays which arrive the concentrator it will be parallel to its axis. The bending surface of parabolic will concentrate whole the rays to a focal point, a trough usually expands the shape with three dimensions to extend focal point to a focal line. Along the focal line a receiver is installed. Eq.(2-2) shows the significant link between the width and depth, and Eq.(2-3) is used to calculate the focal point as shown below [32].

$$y = \frac{1}{4.f}x^2 \quad (2.1)$$

$$f = \frac{w^2}{16.a} \quad (2.2)$$

To determine the focus dimension it is needed to specify the depth of collector trough a . And width of the collector w , as shown in figure (2-3). Then start to calculate the focus length from the equation (2.3). All dimensions that determined like length l , width w and the depth collector trough a are specified experimentally according to make the suitable design with the space available and the cost of the module.

At this point it is possible to draw the shape of the collector by use auto cad program with the formula as drawing (2.2).

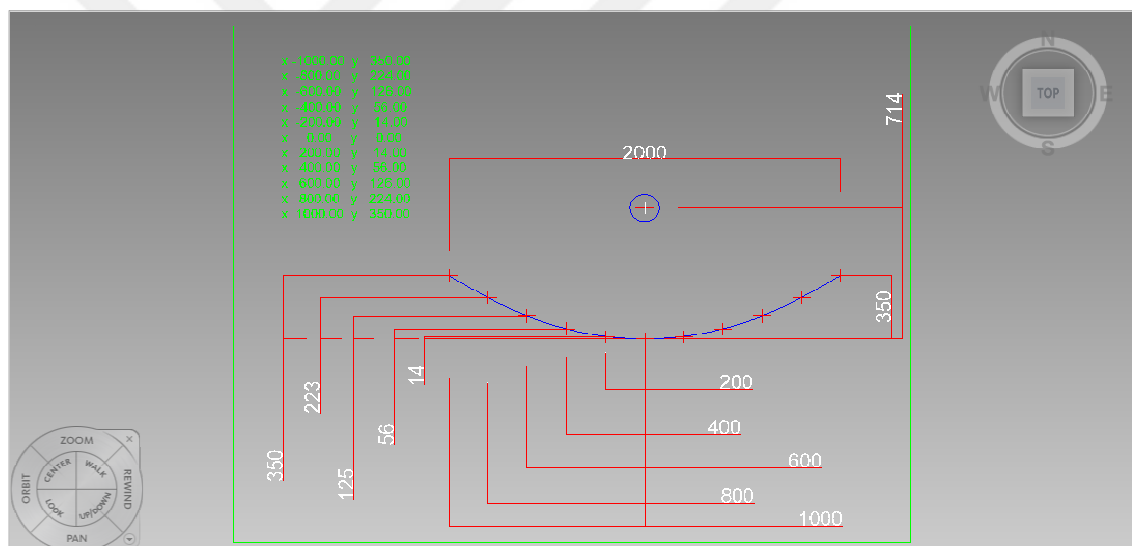


Figure 2. 2 Cross section parabolic collector profile.

The other important parameter which it could specify the shape of collector is the rim angle ψ is the angle between the visual axis and the line connected the focal point with mirror edge as shown in equation (2-3).

It has special properties which it alone could specify the cross-section form for parabolic trough. It means the parabolic troughs with the same rim angle have similar geometrically cross-sections by a regular scale (enlarging or shrinking) [31].

$$\psi = \tan^{-1} \cdot \frac{w/2}{f - a} \quad (2.3)$$

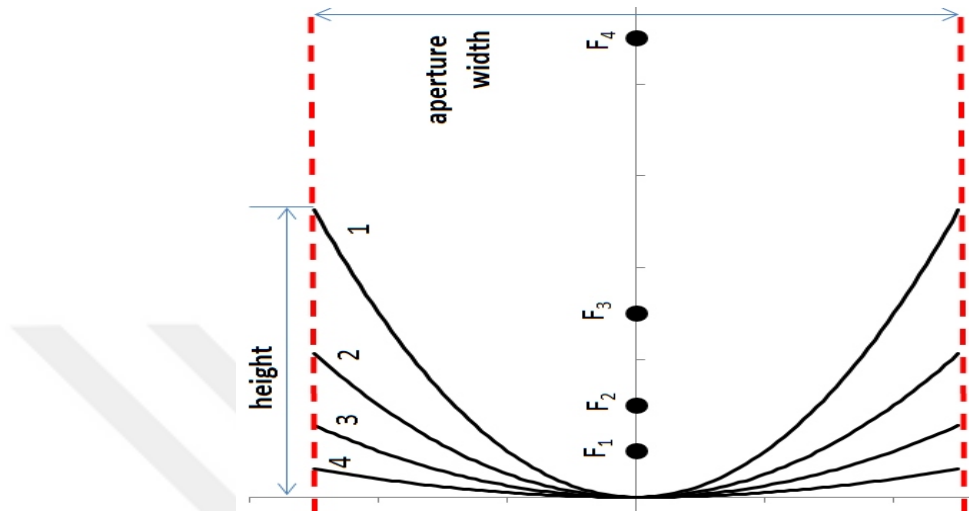


Figure 2. 3 Variation of parabolic curvature and focal distance for fixed aperture.

It is important now to get one of the significant collector variables it is concentration ratio. This is crucial for the potential working temperatures for parabolic power plant that it could raise working temperature by raise this ratio. this ratio can describe as influx radiant intensity on the focal line, relative to the beam radiation enter the collector aperture .and normally it can used the ratio between aperture area to receiver area which is the area concentration ratio [31] [43].

$$C = \frac{A_a}{A_r} = \frac{a.l}{\pi.d.l} = \frac{a}{\pi.d} \quad (2.4)$$

The system and Collector parameters can show in the table below

Table 2. 1 Show the collector and system parameters

Parameters	Value
Collectors dimensions	$W = 2\text{m} , L = 2\text{m}$
Absorb diameter	inside = 0.027 m, outside = 0.031
COVER diameter	0.05
Rim Angle	70
Concentration Ratio	10.6
Receiver Emittance (ϵ_r)	0.1
Cover Emittance (ϵ_c)	0.88
Inside Temp. (T_i)	$45\text{ }^\circ\text{C} = 393\text{ k}$
Ambient temp. (T_a)	$10\text{ }^\circ\text{C} = 293\text{ k}$
Heat transfer coefficient inside the tube (h_{fi})	$300\text{ w/m. }^\circ\text{C}$
Conductivity of pipe receiver for st.st. pipe (k)	$16\text{ w/m. }^\circ\text{C}$
Reflectivity of the reflector (ρ)	0.85
Mass flow rate (\dot{m})	0.05 kg/s
Specific heat with constant pressure (c_p)	4180
the tilted angle (β)	15°
surface reflect ρ	0.8
transmittance glass cover τ	0.95
absorbance the absorber α	0.9

2.1.2 Collector Solar Radiation Calculations

In this section, solar radiation is calculated theoretically according to the equations in Chapter (1). And make changes that would be appropriate with the experience circumstance. The results are used to calculate the heat gain and the total amount of steam that the collector must theoretically receive in this experiment.

In our experiment, the collector is installed directly to the southward direction of 15 degrees with the polar axis of the Earth to the south, which means that it needs to use the angle of the whole slant (β) in the equations.

Because the increase in heat in this method depends on the concentration of solar radiation energy (CSP), which depends mainly on beam radiation only because the diffuse radiation is not included in the calculations which means that the permeability calculations in the atmosphere must be used to obtain beam radiation τ_b in the equation to obtain Accuracy results from collector performance. First the solar radiation calculation should be done solar radiation (G_b) which is used in thermal gain equations. The amount of heat gain per hour is then calculated to be used to calculate compound efficiency.

To calculate the instance solar beam radiation (G_b) on the experimental collector and refer to Eq. (1.17a), (1.12), (1.22) it can used the eq. below

$$G_b = \tau_b G_{sc} \cdot \left(1 + 0.033 \cos 360 \frac{n}{365}\right) \cdot (\cos(\phi - \beta) \cdot \cos \delta \cdot \cos \omega + \sin(\phi - \beta) \cdot \sin \delta). \quad (1.6)$$

The solar constant, $G_{sc} = 1367 \text{ w/m}^2$.

The atmospheric transmittance for beam radiation τ_b is given form Eq. (1.19)

$$\tau_b = a_0 + a_1 \exp\left(\frac{-K}{\cos \theta_z}\right)$$

The constants (a_0 , a_1) and K for the standard atmosphere are given from equations. (1.19a), (1. 19b), (1. 19c)

$$a_0 = 0.4237 - 0.00821(6 - A)^2$$

$$a_1 = 0.5055 + 0.00595(6.5 - A)^2$$

$$k = 0.2711 + 0.01858 (2.5 - A)^2$$

Where (A) is represent the altitude of the observer in kilometers. The altitude for Kayseri city is 1054 m and it is used 1.054 km in this equation.

The number of the day in year (n) is represented the day of the experiment and refers to table (1.1), n = 324.

$$\cos \theta z = \cos(\phi - \beta) \cdot \cos \delta \cdot \cos \omega + \sin(\phi - \beta) \cdot \sin \delta \quad (1.12)$$

The latitude angle (ϕ)for Kayseri city is $38^{\circ} 43' 55''$ N and it is used in this eq. (38.732)N.

The angle of tilted surface (β) is represent the slop of the collector in this experiment which is tilted to south with 15° . Thus the tilted angle (β) = 15° .

The declination angle (δ) can find from eq. (1.3) with table no. (1.1), number of day= 324.

$$\delta = 23.45 \cdot \sin \left(360 \cdot \frac{284 + n}{365} \right)$$

The hour angle (ω) for Kayseri city can find it out from the equations eq. (1.4), eq. (1.5), eq. (1.6), eq. (1.7)

$$\omega = 15^{\circ} \cdot (\text{Solar time} - 12)$$

The solar time for Kayseri city can find from eq. below

$$\text{Solar time} = \text{standard time} + 4(L_{st} - L_{loc}) + E$$

The **Standard time** for Kayseri city which is same of turkey is (+3)

Where L_{loc} is the longitude of the local standard time meridian of Kayseri and turkey is 45°

Where L_{st} is the longitude site of Kayseri ($35^{\circ} 29' 07'' E$) and it is used in this eq. (35.485 E).

E is the adjustment equation of time (in minutes) from eq. bellow

$$E = 229.2 (0.000075 + 0.001868 \cos B - 0.032077 \sin B - 0.014615 \cos 2B - 0.04089 \sin 2B)$$

Where (B) is found from Equation bellow and (n) is number day of year.

$$B = (n-1) \cdot \frac{360}{365}$$

2.1.3 The Collector Heat Losses

Heat losses are significant variable that could influence in direct way at collector efficiency. decreasing the Heat loss of parabolic solar collector is crucial since it will raise the collector efficiency .when the solar energy resource transmit to the absorber surface of collector, it increases the absorber surface temperature higher than the ambient temperature. That is lead to begin heat loss process from receiver like each heated surface with temperature more than ambient temperature. The mechanisms of losses are convection, radiation and conduction.

In our study the annulus gap is evacuated therefore the heat transfer Convection can neglected between the cover and receiver.

First of all it is needed to find the heat losses (Q_{loss}) then it can find the heat losses coefficient (U_l) which is important in the heat useful equation.

The receiver used in this experiment is a compound of stainless steel receiver tube with 40 mm diameter covered by glass cover with 60 mm diameter and 4 mm thickness and the glass evacuated to reduce the heat losses transferred. This tube receiver is designed to increase the heat radiation absorbed and decrease the surface emittance.

Equation (2.5) can be adopted to calculate the heat lose assuming that the temperature of the glass cover is the same as the ambient temperature. And the equation can be written as

$$Q_{loss} = \frac{\pi \cdot D_r \cdot L \cdot \sigma \cdot (T_r^4 - T_a^4)}{\frac{1}{\epsilon_r} - \frac{1 - \epsilon_c}{\epsilon_c} \left(\frac{D_r}{D_{ci}} \right)} \quad (2.5)$$

The heat loss coefficient (based on receiver area) is found from the definition given by Equation (2.6) [16] [36].

$$U_L = \frac{Q_{\text{loss}}}{\pi \cdot D_r \cdot L \cdot (T_r - T_a)} \quad (2.6)$$



2.1.4 The Collector Heat Gain and Theoretical Efficiency.

Average useful gain of heat (Q_u) is the amount of thermal energy that is absorbed in the tube by the flow fluid. The difference between absorbed solar radiation and heat loss is the beneficial energy output of a collector.

In this section, many equations are used to get the heat useful of the collector by make balancing between the optical absorbed heat and thermal heat loss. Then it is need to identify many important properties that have a direct impact on the collector performance. After that it could compare the results with actual heat gain by the collector in the experiment to assess the efficiency of the collector. The main equation explain this description eq. (2-7) [16][38] [39].

$$Q_u = A_{ap} \cdot F_R \left[S - \frac{A_r}{A_{ap}} U_L (T_i - T_{amb}) \right] \quad (2-7)$$

The outside surface area of the tube receiver can get by

$$A_r = \pi \cdot D_r \cdot L \quad (2-7a)$$

The aperture area can get as the following

$$A_{ap} = W \cdot L$$

The absorbed radiation by receiver per unit area (S) is get from the direct solar radiation. Nevertheless, this solar source is decreased via many losses since it moves from collector aperture to the receiver. The amount of optical energy that arriving to the receiver is the result of the solar source that influx multiplied by many factors that reflecting collector surfaces, part of radiation of reflected is intercepting by the receiver that is called intercept factor(γ), absorbance of surface receiver , glass cover transmittance , all less than 1.0 this decrease represent as the following[35] [16] [43].

$$S = G_b \cdot \rho \cdot \gamma \cdot \tau \cdot \alpha \quad (2-8)$$

The beam solar radiation (G_b) can be used from eq. (2.6) as the date and time of the experiment.

The other important factors that are needed in this equation are F' , F_R .

Collector efficiency factor (F'), defined as the ratio of the real useful energy gain to the useful energy that could result if the collector absorbing surface had been at the local fluid temperature [43].

The collector efficiency factor rises when there is a rise in both convection heat transfer coefficient and thermal conductivity, while it decreases when the overall heat loss coefficient [16] [37].

The collector efficiency is given as

$$F' = \frac{1/U_1}{\frac{1}{U_1} + \frac{D_o}{h_{fi} D_i} + \left(\frac{D_o}{2K} \ln \frac{D_o}{D_i}\right)} \quad (2.9)$$

Collector heat removal factor (F_R), represents the traditional heat exchanger activity, which describes the rate of the real heat transfer to the highest potential heat transfer.

The extreme possible useful energy gain in a solar collector happens when the entire collector is at the inlet fluid temperature and the heat losses to the surroundings are at the minimum [43].

When the mass flow rate in the collector is increased, the temperature in the collector is reduced. This results in fewer losses because the medium collector temperature is lower and there is a rise in the useful energy gain. This rise is reflected by an increase in the collector heat removal factor F_R because the mass flow rate is increased [38] [39].

The collector heat removal factor is the highest possible while the useful energy gain is equivalent to the real useful energy gain Q_u , and it is represented as:

$$F_R = \frac{\dot{m} \cdot C_p}{A_r \cdot U_1} \left[1 - \exp\left(-\frac{A_r \cdot U_L \cdot F'}{\dot{m} \cdot C_p}\right) \right] \quad (2.10)$$

It is suitable to describe the collector flow factor F'' as the ratio of F_R to F' Thus

$$F'' = \frac{F_R}{F'} = \frac{\dot{m} \cdot C_p}{F' \cdot A_r \cdot U_l} \left[1 - \exp \left(- \frac{A_r \cdot U_l \cdot F'}{\dot{m} \cdot C_p} \right) \right] \quad (2.10a)$$

The final step in this item to estimate of collector performance is measuring the collector theoretical efficiency, which is describe as the rate of the useful heat gain by collector from equation (2.7) to the incident solar energy from experiment device [40][41].

The theoretical thermal efficiency is writing as

$$\eta_{th} = \frac{Q_{u,th. \text{ by col.}}}{A_c \cdot G_b} \quad (2.11)$$

$$\eta_{th} = \frac{A_{ap} \cdot F_R \left[S - \frac{A_r}{A_{ap}} U_L (T_i - T_{amb}) \right]}{A_{ap} \cdot \tau_b G_{sc} \cdot \left(1 + 0.033 \cos 360 \frac{n}{365} \right) \cdot (\cos(\phi - \beta) \cdot \cos \delta \cdot \cos \omega + \sin(\phi - \beta) \cdot \sin \delta)} \quad (2.12)$$

2.1.5 The Collector Steam Generation.

At this stage, the amount of steam that can be obtained from the collector used in the experiment must be calculated. Before this step. The heat useful increases the temperature of the liquid (water) inside the collector until it reacts the water boiling temperature under pressure (0.1 map), then in this case the heat useful will change the state of water to steam.

The same way of calculate the heat gain will be used to find the quantity of the steam that can get it from the collector by the following.

At the first time, it should calculate the heat useful from the equation (2-7). Then it must note that in this case the collector removal factor should not take in the calculation because there is no gradation in temperature inside the collector and the water in the collector is equal in all parts, that mean only the efficiency collector factor can use in heat gain equation (2-7) and it can written as[16].

$$F_R = F'$$

$$Q_u = A_{ap} \cdot F' \left[S - \frac{A_r}{A_{ap}} U_L (T_i - T_{amb}) \right] \quad (2.13)$$

From the vapor charts it must find the heat enthalpy of the water (h_f), (h_g) at temperature 99.6 c° and (0.1 Mpa.) pressure, and find the heat gain from eq. (2.11) then find the theoretical quantity of the steam as equation below

$$\dot{m}_{\text{steam,th.}} = \frac{Q_u}{h_g - h_f} \quad (2.14)$$

2.1.6 The Calculation by Excel Program.

The final section of the theoretical part is to make an excel program that do the calculations automatically by use the equations which mentioned in this research. This program can divided in three main sections classified according to the required procedures.

The first one used to calculate the beam radiation reach to the earth per one square meter and include all the equations and information regarding to this subject as shown in the figure (2-4).

THE BEAM RADIATION CALCULATIONS					
standard time	Beam Radiation (Gb)	cos zenth angle	The declination angle (δ)	The hour angle (ω)	Solar time
	$G_b = T_b \cdot G_{sc} \cdot (1 + 0.033 \cos 360 \cdot n/365) \cdot \cos(\phi - \beta) \cdot \cos \delta \cdot \cos \omega + \sin(\phi - \beta) \cdot \sin \delta$	$\cos \theta_z = \cos(\phi - \beta) \cdot \cos \delta \cdot \cos \omega + \sin(\phi - \beta) \cdot \sin \delta$	$\delta = 23.45 \cdot \sin(360 \cdot (284 + n)/365)$	$\omega = 15 \cdot (\text{solar time} - 12)$	$\text{solar time} = \text{standard time} + 4(Lst - Lloc) +$
8	56.51077185	0.136472945	-23.09609693	-69.59027629	7.360648247
9	228.7205033	0.330607057	-23.09609693	-54.59027629	8.360648247
10	406.603796	0.491496035	-23.09609693	-39.59027629	9.360648247
11	543.2355786	0.608186674	-23.09609693	-24.59027629	10.36064825
12	620.393387	0.672734757	-23.09609693	-9.59027629	11.36064825
13	630.029563	0.680745897	-23.09609693	5.40972371	12.36064825
14	571.2060158	0.631674701	-23.09609693	20.40972371	13.36064825
15	478.2352362	0.631674701	-23.09609693	35.40972371	14.36064825
16	280.7091574	0.379306921	-23.09609693	50.40972371	15.36064825
17	98.1964014	0.193191355	-23.09609693	65.40972371	16.36064825
	W/m ² .Sec.	non	degree	degree	hour

The atmospheric transmittance	the radiation absorptance of receiver	time coefficient	The adjustment time	The atmosphere factors
$\tau_b = a_0 + a_1 \exp(-k/(\cos \theta_z))$	$S = G_b \cdot \rho \cdot \tau \cdot \alpha$	$B = (n - 1) \cdot 360/365$	$E = 229.2 (0.000075 + 0.001868 \cos B - 0.032077 \sin B - 0.014615 \cos 2B - 0.04089 \sin 2B)$	$a_0 = 0.4237 - 0.00821(6 - A)^2$
0.293235022	38.65336794	318.5753425	14.12482473	0.22285946
0.489918842	156.4448242			$a_1 = 0.5055 + 0.00595(6.5 - A)^2$
0.585844792	278.1169964			0.68197055
0.632531954	371.5731358			$k = 0.2711 + 0.01858 (2.5 - A)^2$
0.653062066	424.3490767			0.309949219
0.65540094	430.9402211			
0.640369226	390.7049148			
0.640369226	327.1129015			
0.524079265	192.0050637			
0.359947406	67.16633855			
non	W/m ² .Sec.			

Figure 2. 4 The beam radiation calculation.

The second section of this program is to compute the collector heat useful, the collector theoretical efficiency and the amount steam that could get from the collector as shown in figure (2-5).

THE COLLECTOR CALCULATIONS (HEAT GAIN & EFFICIENCY)									
Time	S= absorbed radiation	ambient Temp	inside temp.	D=aperture	Q= heat useful gain	Aa=ape	FR= collector	Ar=reci	UL=losses
time	S= absorbed radiation	ambient temp.(k)	inside temp.(k)	D=aperture length	Qu = Aa*FR*((S-(Ar/Aa)*UL*(Ti-Ta))	Aa=D*L	FR= F''*F'	Ar=n*a*L	UL=QL/(Ar*(Ti-Ta))
08:00	38.65336794	274	275	2	154.0158567	4	0.996898446	0.16956	0.698516271
09:00	156.4448242	275	276	2	623.6978221	4	0.996864532	0.16956	0.706178156
10:00	278.1169964	277	278	2	1108.78163	4	0.996795969	0.16956	0.721669601
11:00	371.5731358	279	282	2	1480.996795	4	0.99669119	0.16956	0.74534794
12:00	424.3490767	280	292	2	1689.839224	4	0.996491969	0.16956	0.790382359
13:00	430.9402211	282	299	2	1715.04262	4	0.996322855	0.16956	0.828625145
14:00	390.7049148	282	305	2	1553.567435	4	0.996205625	0.16956	0.855142707
15:00	327.1129015	282	314	2	1298.405081	4	0.996023787	0.16956	0.896286788
16:00	192.0050637	281	316	2	759.6219268	4	0.996001619	0.16956	0.901303762
17:00	67.16633855	279	311	2	262.9289852	4	0.996141986	0.16956	0.869540409
hour	W/m^2.Sec.	k	k	m	w	m^2	non	m^2	W/m^2.c

QL=heat losses	F'=collector efficiency	F''=collector flow factor	collector theoretical efficiency	Qu kw/hour	Steam Produce
$QL=Ar*o*(Ti^4-Ta^4)/((1/cr)+(1-c)c)/(Dr/Dci)$	$F'=1/UL*((1/UL)+(Do/Hf/Di)+(Do/2K*ln(Do/Di)))$	$F''=(rhc/(Ar*UL*F'))*(1-EXP(-(Ar*UL*F'))/(rhc))$	$\eta = Qu/Gb*Aa$	$Qu(kw/hr) = Qu*3.6$	$\dot{m} = (Qu Kw/hr)/(hg - hf)$
0.118440419	0.997180148	0.999717502	0.68135619	554.4570843	0.25
0.119739568	0.997149306	0.999714413	0.681724871	2245.31216	0.99
0.122366298	0.997086952	0.999708167	0.681733447	3991.613868	1.77
0.37914359	0.996991661	0.999698623	0.681562868	5331.588463	2.36
1.608206793	0.996810475	0.999680475	0.680954721	6083.421205	2.69
2.388528554	0.996656665	0.99966597	0.680540634	6174.153434	2.73
3.33495394	0.996550041	0.999654391	0.679950575	5592.842767	2.48
4.863180407	0.996384651	0.999637827	0.678748126	4674.258291	2.07
5.348877306	0.996364488	0.999635807	0.676520436	2734.638936	1.21
4.718056693	0.996492159	0.999648594	0.669395674	946.5443468	0.42
W	non	non	non	Kw/hr	Kg

Figure 2. 5 Collector calculations heat gain, theoretical efficiency & amount steam.

The third section in this program calculate the actual heat gain by experiment and the collector experimental efficiency as shown in figure (2-6).

THE EXPERIMENTAL CALCULATIONS			
tem. out of tube	tem. inside tube	heat gain experimentaly	collector experimentally efficiency
Tout	Tin	Qexp=rhc*(Tout-Tin)	$\eta = Qexp/Gb*Aa$
0	0	0	0.00
0	0	0	0.00
0	0	0	0.00
10.8	9.4	292.6	0.22
20.3	19.1	250.8	0.17
32	29.8	459.8	0.30
42	38	836	0.61
49.8	46.1	773.3	0.67
40.3	38.7	334.4	0.50
0	0	0	0.00
k	k	w	

Figure 2. 6 Experimental calculation (heat gain & experimental efficiency).

The fourth section of this program is to compute the sun altitude angle (α) hourly per number of day in a year as figure (2-7).

SUN hourly raise per no. day of year (α)	
SUN ALTITUDE FACTOR	SUN RAISE ANGLE (α)
$x = ((\cos \phi) \cdot \cos (\delta) \cdot \cos (\omega) + \sin$	$\sin^{-1}(x)$
0.04	2.31
0.21	12.07
0.35	20.43
0.45	26.77
0.51	30.44
0.51	30.90
0.47	28.09
0.38	22.43
0.25	14.56
0.09	5.14

Figure 2. 7 Show sun altitude angles (α) hourly per number of day per year.

It should note there is some data should be filled into table to could get the results demanded (2-8).

DATAShould FILL IN			
Data required for collector	the value	amb. tom. Required (8:00-15:00)	inside temp. required (8:00-15:00)
receiver tube diameter(out) (m)	0.027	274	275
length of tube & aperture L (m)	2	275	276
emittance of receiver (ϵ_r)	0.15	277	278
emittance of cover (ϵ_c)	0.88	278	283
receiver tube diameter (in) (m)	0.023	280	293
glass cover diameter (in) (m)	0.075	281	304
heat transfer coefecient (hfi)	300	281	313
conductivity of pipe receiver (k)	16	280	321
water flow rate (m)	0.05	279	312
constant pressure (cp)	4180	278	305
enthalpy of vapour water (hg)	2675		
enthalpy of fluid water (hf)	417		

Data required for radiation	the value	collector outlet. temp. (8:00-15:00)	collector inlet temp. (8:00-15:00)
latitude angle (ϕ) of the the city	38.732	0	0
collector surface slop angle (β)	15	0	0
number of day (n)	343	0	0
the longitude site L_{st}	35.485	10.8	9.4
longitude local standard time L_{loc}	45	20.3	19.1
A= altitude in km	1.054	32	29.8
The surface reflected (ρ)	0.8	42	38
The transmittance of glass cover (τ)	0.95	49	46.1
The absorptance of absorber (α)	0.9	40.3	38.7
		0	0

Month	n for i:th Day of Month	For the Average Day of the Month	
		Dayc	δ Day of Year Declination
January	i	17	17 -29.9°
February	31+i	16	47 -13.0°
March	59+i	16	75 -2.4°
April	90+i	15	105 9.4°
May	120+i	15	135 18.3°
June	151+i	11	162 23.1°
July	181+i	17	198 21.2°
August	212+i	16	228 13.5°
September	243+i	15	258 2.2°
October	273+i	15	288 -9.6°
November	304+i	14	318 -18.9°
December	334+i	10	344 -23.0°

Figure 2. 8 Data need to fill in for collector theoretically, experimentally and radiation.

2.2 Experimental thermal performance of (PTC).

In this section, the experimental performance of the (PTC) is studied to understand the behavior and the experimentally efficiency of the collector in two phases. The first one is heating water to raise its temperature to the boiling degree. The second stage is boiling the water to evaporate it and produce the steam. The experiment must do in a two separated cycles then it should compare the experimental results with the theoretical result and estimate the different between them.

2.2.1 Experimental Collector Manufacture and Install.

The solar collector which consists of a parabolic section curve was drawn by using AutoCAD according to the equation ($y=x^2/4F$) as shown in fig (2.1). The curve frames manufactured by use special CNC machine to get the accurate parabolic surface reflector shape before welded with profiles structure in the workshop of Erciyes University as shown in (2.4). Then a special metal bright steel chrome sheet with high reflected ratio rolled and riveted over the reflected shape.

A steel tube receiver paint with black color to receive all the radiation without reflection rays. This receiver covered with an insulated glass tube evacuated from air to insulate the receiver from the ambient, this receiver compound installed in the focus line of the surface reflector.

The receiver connected with pipe net system insulated with glass wool which has a pump to rotate the water in the collector and thermo cables to record the temp in and out of the collector. The solar collector and the receiver are hang by ball bearing let the compound rotate around the axial with the sun direction by a belt connect with gear motor driver work with computer follow program to put the aperture collector direct face the sun radiation beam all the time from the east when sun rise to west when sun set. The whole arrangements are fitted on a steel frame.

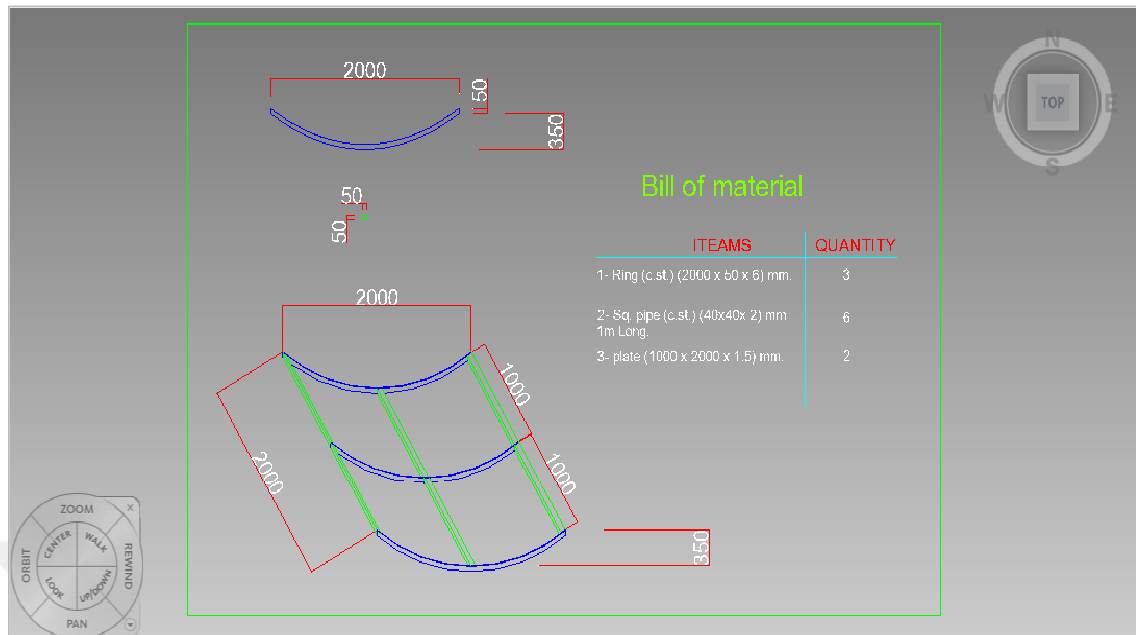


Figure 2. 9 Design the collector profile arrangements from steel structure.

2.2.2 The Experiment Description.

The solar collector system is designed and manufactured to produce the steam by use two stages that because we are treat with two phases of the water liquid and gas.

The two stages are separated to two cycles by used the valves. The first stage is starting with rotating the fluid in the collector system by the pump and pushed it inside the tube receiver to absorb the heat energy transferred by the sun which it is collected by the parabolic collector surface and reflect it to the receiver tube. That it is working to raise its temperature from the inlet temperature to the boiling temperature (99.6 c°).

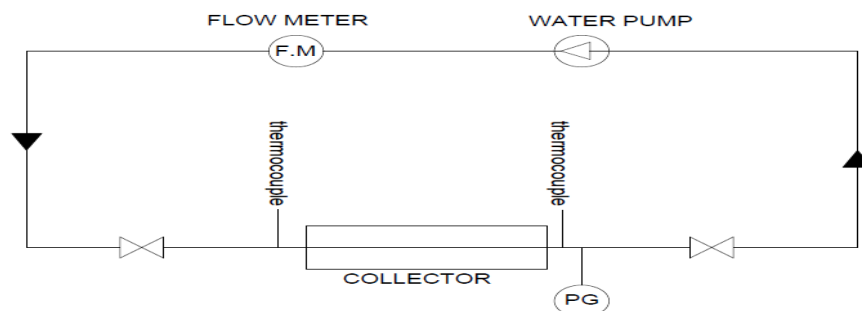


Figure 2. 10 The first stage of hot water rotated in the system.

The insulated pipes work to keep the water temperature and reduce the heat losses from the system. The motor connected with the surface reflected is working to keep the surface facing to the sun direction all the time. The motor take the signal to keep its movement with sun by the electronic driver unit. At this time the recorder work to register of the inlet and outlet temperatures which it connected with two thermo cables which they laid before and after the receiver tube as shown in the figures from (2-5) to (2-17) which is illustrated the exterminate steps. During that it should register the time needed to get the boiling degree to can find the heat gaining with time by use the equation (2.19)[41]. After measure the mass flow rate of the water rotate in the system (\dot{m}) that act to estimate the collector efficiency by comparing with theoretical calculation.

$$\dot{Q}_{\text{use.expl}} = \dot{m} c_p (T_{\text{out}} - T_{\text{in}}) \quad (2.15)$$

The second stage start when the water temperature arrive to the boiling degree (99.6 c°) at this point it should stopped the water rotation by make shutdown to the pump and close the two valves before and after the receiver tube to trap the water inside the tube. The slop of the collector (15°) with the horizontal can help to trap the water inside the tube. Then it must start to register the time need to convert the water to steam by open the vent tube which is connected after the receiver tube to let the steam inside the tube to vent outside the tube.

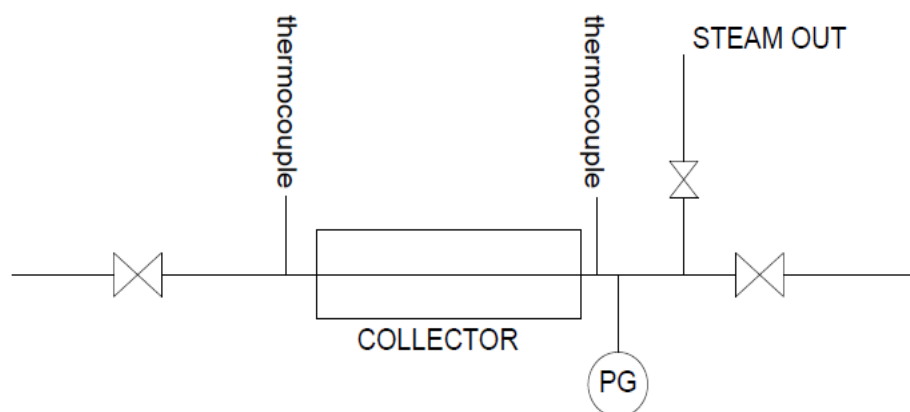


Figure 2. 11 The second stage of producing steam in the system

It could estimate the time it needed to this converted from the theoretical calculations (Eq.2-20). After this time is exhausted it could open drain which is connected before the receiver tube to measure the water still inside the tube and didn't evaporate to can specify the actual evaporating water. Then it could find the collector efficiency to generate the steam and comparing it with the theoretical calculations.

$$\Delta t_{evap,th} = \frac{m (h_g - h_f)}{\tau_b G_{sc} \cdot \left(1 + 0.033 \cos 360 \frac{n}{365}\right) \cdot (\cos(\phi - \beta) \cdot \cos \delta \cdot \cos \omega + \sin(\phi - \beta) \cdot \sin \delta)} \quad (2-16)$$

m: is the quantity of water trapped inside the tube it cold measure before filling it.

Where $h_g = 2675$ kJ/kg , $h_f = 417.4$ kJ/kg at 99.6 c°, $P = 0.1$ Mpa.



Figure 2. 12 Collector turn to the east at the morning.



Figure 2. 13 Collector turn to the west at the evening and program register temperatures.



Figure 2. 14 The reflected radiation focused on tube receiver.



Figure 2. 15 Adjustment water pump



Figure 2. 16 Flow meter



Figure 2. 17 Thermo cable temperature reader



Figure 2. 18 Ambient temperature indicator



Figure 2.19 Pressure gauge & thermo cable



Figure 2.20 Instrument to measure radiation



Figure 2.21 Collector driver motor



Figure 2.22 Piping insulation



Figure 2. 23 Manufacturing collector system in Erciyes University.



Figure 2. 24 Installs the piping system.

2.2.3 The Experiment Efficiency.

In this section it could estimate the collector efficiency in two parts.

The first part represent the experimental efficiency of heat gain by the water rotates in the system to the heat gain theoretically by equations in specified time. That is done by

measure the mass flow rate in the system and inlet and outlet temperatures for specified time to the incident solar energy from experiment device [42] [43].

$$\eta_{\text{exp.}} = \frac{Q_{\text{u,exp.}}}{A_{\text{c}} \cdot G_{\text{b}}} \quad (2-17)$$

$$\eta_{\text{exp.}} = \frac{\dot{m} \text{ cp } (T_{\text{out}} - T_{\text{in}})}{A_{\text{c}} \cdot G_{\text{b}}} \quad (2-17\text{a})$$

$$G_{\text{b}} = G_{\text{I}} (1 - \tau_{\text{d}})$$

$$\tau_{\text{d}} = 0.271 - 0.294 \tau_{\text{b}} \quad (1-21 \text{ a})$$

Where(G_{I}) the total heat radiation measures by radiation device experimentally.

The second part is estimate the evaporated experimental efficiency of collector by knowledge the ratio of the actually steam mass quantity generated by collector in the experiment to the beam radiation and the theoretical efficiency of collector find by get the ratio of steam generator theoretically to the beam radiation.

$$\eta_{\text{steam,exp.}} = \frac{m_{\text{exp.}} \cdot h_{\text{fg.}}}{A \cdot G_{\text{b.}}} \quad (2-18)$$

$$\eta_{\text{steam,th}} = \frac{m_{\text{th.}} \cdot h_{\text{fg.}}}{A \cdot G_{\text{b.}}} \quad (2-18 \text{ a})$$

CHAPTER 3

RESULT AND DISCUSS

3.1 Collector Theoretical Efficiency Result Analysis

In this section it will check and analysis the collector results according to the properties that impact direct and indirect on the system and study how can control these properties to improve the system efficiency.

3.1.1 Collector Efficiency with Aperture Dimensions

With this point of investigation, it could use the excel program by change the aperture dimensions and check the change will happen with results to can estimate the performance of the collector with change the aperture dimensions as the figures bellow.

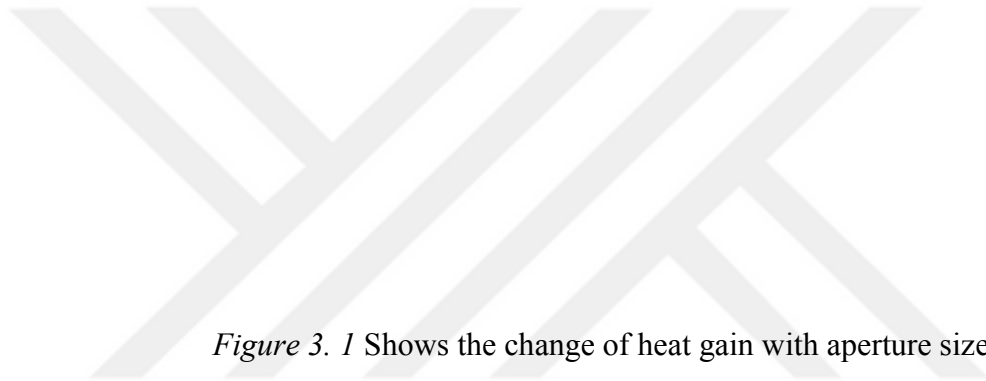


Figure 3. 1 Shows the change of heat gain with aperture sizes

By use the excel program to calculate the heat gain and the collector efficiency it could show from Figure (3-1) above the change of increasing the heat gain by increasing the aperture size. The heat gain is 1105 w/m^2 for aperture size 2 m (experimental chose).

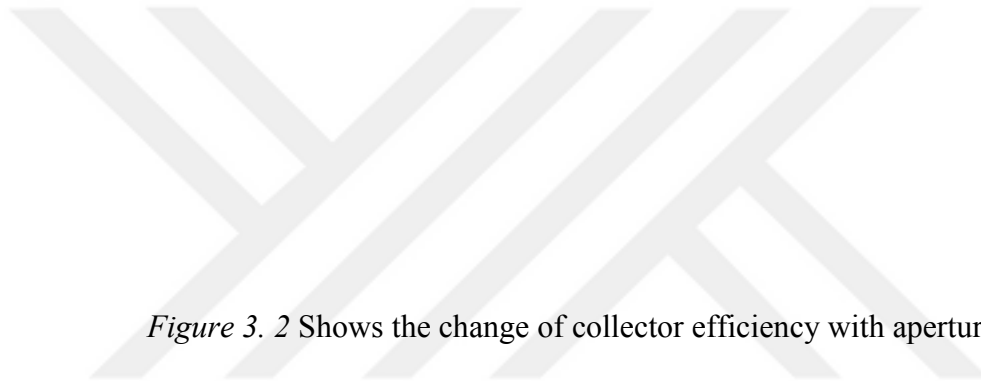


Figure 3. 2 Shows the change of collector efficiency with aperture sizes

However, at the same time it could be obvious a small change of the collector efficiency as shown in figure (3-2) which is because of increase the concentrated ratio (A_r/A_a) as in eq.(2-12) and that it could increase the impact of the collector efficiency at the high collector temperatures cases. Theoretical efficiency is 0.6272 for aperture size is 2 m.

3.1.2 Collector Efficiency Change With receiver Tube Diameter.

The other important geometrical property that could impact to the efficiency of the collector is the diameters of receiver tube which it is investigated in this point to check how this property can impact of the collector efficiency by use the excel program and the charts as shown below:

Figure 3. 3 Shows change of receiver diameter with collector efficiency & flow factor

By study the results from the program and the figure (3-3) above it could observe that the increasing of the collector receiver tube lead to decrease the collector efficiency in our case the tube diameter 0.04m and the tube flow factor is 0.90 and the collector efficiency 0.6.

Figure 3. 4 Shows the change of heat losses with receiver tube radius

and there are two main reasons behind this decreasing in the efficiency the first one is the raising in the heat losses because of the increasing in the tube surface area which is facing to the ambient as shown in figure (3-4) and it could increase with the collector high temperatures degree in our case with tube 0.04 m diameter the heat losses is 1.4 watt. However, the increasing in heat losing is not significant to make a big change in efficiency if the tube emittance is not high. The second important reason which has effect on the efficiency and has a relation with the receiver tube diameter is the collector flow factor (F'). By study the results from the program it could find out that there is inverse relation between the tube diameter and the collector flow factor as the increasing in tube diameter cause decreasing in the collector flow factor which is effect on the efficiency negatively as s shown in figure (3-3).

3.1.3 Collector Efficiency Changes with Flow Rate.

One of the important properties which can impact on the collector efficiency is the mass flow rate which is passes through the collector to transmit the solar energy before converted it to mechanical and electrical energy. The normal fluid used in the solar radiation stations inside the collector is artificial oil which is boiling in a very high temperature to avoid the saturated fluid state. In our experiment we use water as a transmit fluid and it will used the excel program to investigated the changing quantity of the mass flow rate inside the same collector to observe the change that it will happened on the heat gain and efficiency as show in the following drawings.

Figure 3. 5 Shows the change of heat gain with flow rate.

By study the results which are get from the excel program and study the charts graphics above it could observe that when increase the mass flow rate that passes through the collector it leads to increase the heat gain in the collector as shown in the figure (3-5) when other properties be constant in our case the flow rate is 0.3 kg/sec. and the heat gain is 836 watt/m².

Figure 3. 6 Shows the change of flow rate with efficiency & flow factor (F").

And if it checks the figure (3-6) it could observe that the increasing in the mass flow rate lead to increase the collector tube flow rate factor (F'') and that is the reason of increasing in the heat gain in our case ($F'' = 0.925$). (F'') get to the highest level and it will not be able to increase more. In our case the flow rate should be not less than $0.0004m^3/s$ which mass flow rate is (0.4 Kg/s). It could observe more that the change of the efficiency can be significant when there is a big change in the little mass flow rate than the big mass flow rate so the efficiency with our mass flow rate 0.3 kg/se is (0.63).

3.1.4 Collector Efficiency change with Receiver Tube Emittance.

This property has a direct impact of the collector efficiency by a strong relation with heat losses and the collector flow factor it could observe from the figures below.

Figure 3. 7 Shows the change receiver tube emittance with flow factor & efficiency.

The other important properties are the surface of receiver tube emittance which it has a direct impact of the collector efficiency. When study the result from the program and the figure (3-7) it could find that the increasing of the tube surface emittance lead to directly decrease in the collect efficiency in our case receiver emittance (0.1) and the tube efficiency is 0.65 and the flow rate factor is 0.95.

There are two reasons behind this increasing the raising of heat losing as in the figure (3-8) in our case the heat losses is 0.61 watt when emittance is (0.1). And that will be significant in collector high temperatures degree, the other reason behind the collector efficiency decreasing is the decline in collector flow factor (F'') as shown in figure (3-8).



Figure 3. 8 Shows the change of receiver tube emittance with collector heat losses

It is important to mentions here that the increasing in the emittance causes a sharp decreasing in the efficiency when increasing the receiver tube diameter as shown in the Figure (3-9). For 0.1 tube emittance, Tube heat losses is 0.617 W/m².

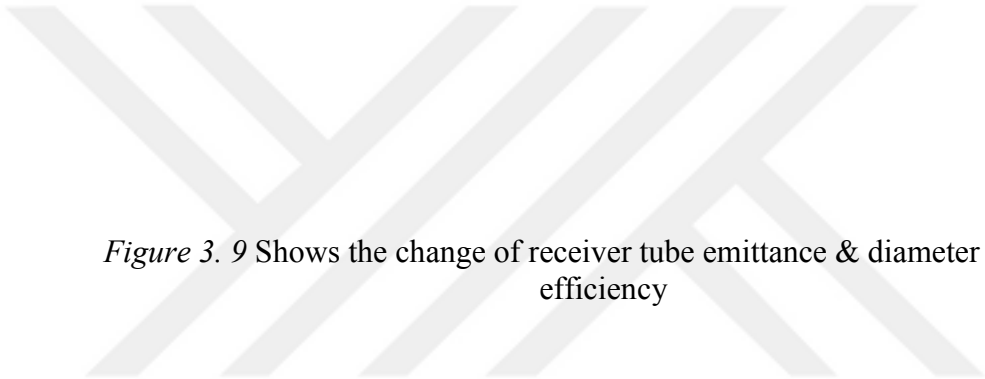


Figure 3. 9 Shows the change of receiver tube emittance & diameter size with efficiency

3.1.4 Collector Efficiency and Indirect Properties.

In this step of the study, some properties that have an indirect effect on the efficiency of the collector such as ambient temperature and liquid temperatures can be mentioned, which have the opposite effect on the efficiency of the collector. The reason is that increasing the difference in temperatures leads to increased heat loss and reduced efficiency. Other indirect properties are experimental properties such as dust and surface dirt that affect the reflection of the radiation from the surface of the compound and the permeability of the pipe, which indirectly affect the efficiency of the collector.

3.1.5 Calculation of Theoretical collector Efficiency.

To calculate the collector efficiency theoretically it could use the following procedures by calculate the solar radiation at the first then calculate the heat gain and the collector efficiency finally as the following.

Theoretical efficiency on 9/12/2018 at 1:00

Theoretical Beam radiation

$$G_{b,th} = \tau_b G_{sc} \cdot \left(1 + 0.033 \cos 360 \frac{n}{365}\right) \cdot (\cos(\phi - \beta) \cdot \cos \delta \cdot \cos \omega + \sin(\phi - \beta) \cdot \sin \delta) \quad (1.20)$$

The solar constant radiation is $G_{sc} = 1367 \text{ w/m}^2$.

$$\text{The Beam transition factor is } \tau_b = a_0 + a_1 \exp\left(\frac{-K}{\cos \theta_z}\right) \quad (1.19)$$

The constants (a_0 , a_1) and K for the standard atmosphere are given from equations: eq. (1.21a), eq. (1.21b), eq. (1.21c). Where (A) = **1.054 km**.

$$a_0 = 0.4237 - 0.00821(6 - A)^2$$

$$a_0 = 0.4237 - 0.00821(6 - 1.054)^2 = \mathbf{0.22}$$

$$a_1 = 0.5055 + 0.00595(6.5 - A)^2$$

$$a_1 = 0.5055 + 0.00595(6.5 - 1.054)^2 = \mathbf{0.68}$$

$$k = 0.2711 + 0.01858 (2.5 - A)^2$$

$$k = 0.2711 + 0.01858 (2.5 - 1.054)^2 = \mathbf{0.31}$$

Cos Zenith Angle

$$\cos \theta_z = \cos(\phi - \beta) \cdot \cos \delta \cdot \cos \omega + \sin(\phi - \beta) \cdot \sin \delta \quad (1.12)$$

The latitude angle (ϕ) for Kayseri city is (**38.732**) N, the tilted angle (β) = 15° .

The declination angle (δ) can find from eq. (1.3) with table no. (1.1),

Day number = 343.

Declination angle

$$\delta = 23.45 \cdot \sin\left(360 \cdot \frac{284 + 324}{365}\right)$$

$$\delta = -22.59$$

–The hour angle (ω) for Kayseri city can find it out from the equations

(1.4, 1.5, 1.6, 1.7)

Hour angle

$$\omega = 15^\circ (\text{Solar time} - 12)$$

$$\text{Solar time} = \text{standard time} + 4(L_{st} - L_{loc}) + E$$

The Standard time for Kayseri city which is same of turkey is (+3), Where L_{loc} is the longitude of the local standard time meridian of Kayseri and turkey is 45° Where L_{st} is the longitude site of Kayseri and it is used in this eq. (35.485 E).

Factor E is the equation of time.

$$E = 229.2 (0.000075 + 0.001868 \cos B - 0.032077 \sin B - 0.014615 \cos 2B - 0.04089 \sin 2B)$$

$$\text{Day number factor } B = (324-1) \times \frac{360}{365}$$

$$B = 337.32$$

$$E = 229.2 (0.000075 + 0.001868 \cos (318.6) - 0.032077 \sin (318.6) - 0.014615 \cos (2 \times 318.6) - 0.04089 \sin (2 \times 318.6))$$

$$E = 7.64$$

$$\text{Solar time} = 1 + 4(35.485 - 45) + 14.1$$

$$\text{Solar time} = 12.30$$

$$\text{Hour angle } \omega = 15^\circ \times (12.361 - 12)$$

$$\omega = 4.44$$

Cos Zenith Angle

$$\cos \theta_z = \cos (38.732 - 15) \cos (-20.18) \cos (5.41) + \sin (38.732 - 15) \sin (-20.18)$$

$$\cos \theta_z = 0.68$$

The Beam transition factor is

$$\tau_b = 0.2229 + \exp(-0.31 / \cos 0.717),$$

$$\tau_b = 0.66$$

Theoretical Beam radiation

$$G_{b,th} = 0.67 \times 1367 \cdot \left(1 + 0.033 \cos 360 \frac{324}{365}\right) \cdot \cos \theta_z$$

$$G_b = 0.67 \times 1367 (1 + 0.033 \cos 360 \frac{324}{365}) 0.717$$

$$G_b = 633 \text{ watt/m}^2.$$

$$\text{Useful beam radiation } S = G_b \cdot \rho \cdot \tau \cdot \alpha \quad (2-8)$$

From table (2.1) surface reflect $\rho = 0.80$, transmittance glass cover $\tau = 0.95$, absorbance the absorber $\alpha = 0.9$

$$S = 668.5 \times 0.74 \times 0.95 \times 0.9$$

$$S = 401 \text{ watt/m}^2.$$

Heat losses at tube

$$Q_{\text{loss}} = \frac{\pi \cdot D_r \cdot L \cdot \sigma \cdot (T_r^4 - T_a^4)}{\frac{1}{\epsilon_r} - \frac{1 - \epsilon_c}{\epsilon_c} \left(\frac{D_r}{D_{ci}}\right)} \quad (2.5)$$

$$Q_{\text{loss}} = \frac{3.14 \times 0.027 \times 2 \times 5.67 \times 10^{-8} \cdot ((309)^4 - (290)^4)}{\frac{1}{0.15} - \frac{1 - 0.88}{0.88} \left(\frac{0.027}{0.05}\right)}$$

$$Q_{\text{loss}} = 2.21 \text{ watt/m}^2.$$

Heat losses coefficient

$$U_L = \frac{Q_{\text{loss}}}{\pi \cdot D_r \cdot L \cdot (T_r - T_a)} \quad (2.6)$$

$$U_L = \frac{2.98}{3.14 \times 0.027 \times 2 \times (309 - 290)}$$

$$U_L = 0.57$$

Useful heat

$$Q_u = A_{ap} \cdot F_R \left[S - \frac{A_r}{A_{ap}} U_L (T_i - T_{amb}) \right] \quad (2-7)$$

Collector efficiency

$$F' = \frac{1/U_1}{\frac{1}{U_1} + \frac{D_o}{h_{fi} D_i} + \left(\frac{D_o}{2K} \ln \frac{D_o}{D_i} \right)} \quad (2.9)$$

$$F' = \frac{1/0.57}{\frac{1}{0.57} + \frac{0.027}{300 \times 0.023} + \left(\frac{0.027}{2 \times 16} \ln \frac{0.027}{0.023} \right)}$$

$$F' = \mathbf{0.9977}$$

Collector flow factor

$$F'' = \frac{F_R}{F'} = \frac{\dot{m} \cdot C_p}{F' \cdot A_r \cdot U_1} \left[1 - \exp \left(- \frac{A_r \cdot U_L \cdot F'}{\dot{m} \cdot C_p} \right) \right] \quad (2.10)$$

$$F'' = \frac{0.05 \times 4170}{3.14 \times 0.027 \times 0.57 \times 0.9977} \left[1 - \exp \left(- \frac{3.14 \times 0.027 \times 0.57 \times 0.9977}{0.05 \times 4170} \right) \right]$$

$$F'' = \mathbf{0.9998}$$

Collector removal factor

$$F_R = F' \times F''$$

$$F_R = \mathbf{0.997}$$

Heat gain by collector

$$Q_u = A_{ap} \cdot F_R \left[S - \frac{A_r}{A_{ap}} U_L (T_i - T_{amb}) \right] \quad (2.7)$$

$$Q_u = 2 \times 2 \times 0.97 \left[401 - \frac{3.14 \times 0.027}{2 \times 2} 0.925 (309 - 290) \right]$$

$$Q_u = 1597 \text{ watt/collector}$$

Theoretical efficiency

$$\eta_{th} = \frac{A_{ap} \cdot F_R \left[S - \frac{A_r}{A_{ap}} U_L (T_i - T_{amb}) \right]}{A_{ap} \cdot \tau_b G_{sc} \cdot \left(1 + 0.033 \cos 360 \frac{n}{365} \right) \cdot (\cos(\phi - \beta) \cdot \cos \delta \cdot \cos \omega + \sin(\phi - \beta) \cdot \sin \delta)} \quad (2.12)$$

$$\eta_{th} = \frac{1597}{4 \times 633}$$

$$\eta_{th} = 0.63$$

Theoretical efficiency on 20/11/2018 at 1:00

Theoretical Beam radiation

$$G_{b,th} = \tau_b G_{sc} \cdot \left(1 + 0.033 \cos 360 \frac{n}{365} \right) \cdot (\cos(\phi - \beta) \cdot \cos \delta \cdot \cos \omega + \sin(\phi - \beta) \cdot \sin \delta) \quad (1.20)$$

The solar constant radiation is $G_{sc} = 1367 \text{ w/m}^2$.

$$\text{The Beam transition factor is } \tau_b = a_0 + a_1 \exp\left(\frac{-K}{\cos \theta_z}\right) \quad (1.19)$$

The constants (a_0 , a_1) and K for the standard atmosphere are given from equations: eq. (1.19a), eq. (1.19b), eq. (1.19c). Where (A) = **1.054 km**.

$$a_0 = 0.4237 - 0.00821(6 - A)^2$$

$$a_0 = 0.4237 - 0.00821(6 - 1.054)^2 = \mathbf{0.22}$$

$$a_1 = 0.5055 + 0.00595(6.5 - A)^2$$

$$a_1 = 0.5055 + 0.00595(6.5 - 1.054)^2 = \mathbf{0.68}$$

$$k = 0.2711 + 0.01858 (2.5 - A)^2$$

$$k = 0.2711 + 0.01858 (2.5 - 1.054)^2 = \mathbf{0.31}$$

Cos Zenith Angle

$$\cos \theta_z = \cos(\phi - \beta) \cdot \cos \delta \cdot \cos \omega + \sin(\phi - \beta) \cdot \sin \delta \quad (1.12)$$

The latitude angle (ϕ) for Kayseri city is (**38.732**) N, the tilted angle (β) = 15° .

The declination angle (δ) can find from eq. (1.3) with table no. (1.1),

Day number = 324.

Declination angle

$$\delta = 23.45 \cdot \sin\left(360 \cdot \frac{284 + 324}{365}\right)$$

$\delta = -20.18$

-The hour angle (ω) for Kayseri city can find it out from the equations

(1.4, 1.5, 1.6, 1.7)

Hour angle

$$\omega = 15^\circ \cdot (\text{Solar time} - 12)$$

$$\text{Solar time} = \text{standard time} + 4(L_{st} - L_{loc}) + E$$

The Standard time for Kayseri city which is same of turkey is (+3), Where L_{loc} is the longitude of the local standard time meridian of Kayseri and turkey is 45° Where L_{st} is the longitude site of Kayseri and it is used in this eq. (35.485 E).

Factor E is the equation of time.

$$E = 229.2 (0.000075 + 0.001868 \cos B - 0.032077 \sin B - 0.014615 \cos 2B - 0.04089 \sin 2B)$$

$$\text{Day number factor } B = (324-1) \times \frac{360}{365}$$

$$B = 318.6$$

$$E = 229.2 (0.000075 + 0.001868 \cos (318.6) - 0.032077 \sin (318.6) - 0.014615 \cos (2 \times 318.6) - 0.04089 \sin (2 \times 318.6))$$

$$E = 14.12$$

$$\text{Solar time} = 1 + 4(35.485 - 45) + 14.1$$

$$\text{Solar time} = 12.36$$

$$\text{Hour angle } \omega = 15^\circ \times (12.361 - 12)$$

$$\omega = 5.41$$

Cos Zenith Angle

$$\cos \theta_z = \cos (38.732 - 15) \cos (-20.18) \cos (5.41) + \sin (38.732 - 15) \sin (-20.18)$$

$$\cos \theta_z = 0.72$$

The Beam transition factor is

$$\tau_b = 0.2229 + \exp(-0.31 / \cos 0.717),$$

$$\tau_b = 0.67$$

Theoretical Beam radiation

$$G_{b,th} = 0.67 \times 1367 \cdot \left(1 + 0.033 \cos 360 \frac{324}{365}\right) \cdot \cos \theta_z$$

$$G_b = 0.67 \times 1367 \left(1 + 0.033 \cos 360 \frac{324}{365}\right) 0.717$$

$$G_b = 673 \text{ watt/m}^2.$$

$$\text{Useful beam radiation } S = G_b \cdot \rho \cdot \tau \cdot \alpha \quad (2-8)$$

From table (2.1) surface reflect $\rho = 0.80$, transmittance glass cover $\tau = 0.95$, absorbance the absorber $\alpha = 0.9$

$$S = 668.5 \times 0.74 \times 0.95 \times 0.9$$

$$S = 426.2 \text{ watt/m}^2.$$

Heat losses at tube

$$Q_{\text{loss}} = \frac{\pi \cdot D_r \cdot L \cdot \sigma \cdot (T_r^4 - T_a^4)}{\frac{1}{\epsilon_r} - \frac{1 - \epsilon_c}{\epsilon_c} \left(\frac{D_r}{D_{ci}}\right)} \quad (2.5)$$

$$Q_{\text{loss}} = \frac{3.14 \times 0.027 \times 2 \times 5.67 \times 10^{-8} \cdot ((309)^4 - (290)^4)}{\frac{1}{0.15} - \frac{1 - 0.88}{0.88} \left(\frac{0.027}{0.05}\right)}$$

$$Q_{\text{loss}} = 11.55 \text{ watt/m}^2.$$

Heat losses coefficient

$$U_L = \frac{Q_{\text{loss}}}{\pi \cdot D_r \cdot L \cdot (T_r - T_a)} \quad (2.10)$$

$$U_L = \frac{2.21}{3.14 \times 0.027 \times 2 \times (372 - 290)}$$

$$U_L = 0.83$$

Useful heat

$$Q_u = A_{ap} \cdot F_R \left[S - \frac{A_r}{A_{ap}} U_L (T_i - T_{amb}) \right] \quad (2-7)$$

Collector efficiency

$$F' = \frac{1/U_1}{\frac{1}{U_1} + \frac{D_o}{h_{fi} D_i} + \left(\frac{D_o}{2K} \ln \frac{D_o}{D_i}\right)} \quad (2.9)$$

$$F' = \frac{1/0.83}{\frac{1}{0.83} + \frac{0.027}{300 \times 0.023} + \left(\frac{0.027}{2 \times 16} \ln \frac{0.027}{0.023}\right)}$$

$$F' = 0.9977$$

Collector flow factor

$$F'' = \frac{F_R}{F'} = \frac{\dot{m} \cdot C_p}{F' \cdot A_r \cdot U_1} \left[1 - \exp\left(-\frac{A_r \cdot U_L \cdot F'}{\dot{m} \cdot C_p}\right) \right] \quad (2.10)$$

$$F'' = \frac{0.008 \times 4170}{3.14 \times 0.027 \times 0.83 \times 0.9977} \left[1 - \exp\left(-\frac{3.14 \times 0.027 \times 0.83 \times 0.9977}{0.008 \times 4170}\right) \right]$$

$$F'' = 0.9986$$

Collector removal factor

$$F_R = F' \times F''$$

$$F_R = 0.996$$

Heat gain by collector

$$Q_u = A_{ap} \cdot F_R \left[S - \frac{A_r}{A_{ap}} U_L (T_i - T_{amb}) \right] \quad (2.7)$$

$$Q_u = 2 \times 2 \times 0.97 \left[426.5 - \frac{3.14 \times 0.027}{2 \times 2} 0.925 (309 - 290) \right]$$

$$Q_u = 1698.4 \text{ watt/collector}$$

Theoretical efficiency

$$\eta_{th} = \frac{A_{ap} \cdot F_R \left[S - \frac{A_r}{A_{ap}} U_L (T_i - T_{amb}) \right]}{A_{ap} \cdot \tau_b G_{sc} \cdot \left(1 + 0.033 \cos 360 \frac{n}{365} \right) \cdot (\cos(\phi - \beta) \cdot \cos \delta \cdot \cos \omega + \sin(\phi - \beta) \cdot \sin \delta)} \quad (2.12)$$

$$\eta_{th} = \frac{1698.4}{4 \times 673}$$

$$\eta_{th} = 0.63$$

3.2 Experimental Collector Efficiency.

In this section it needs to calculate and study the results which it could be get it experimentally from the experiments which they are done by the collector system which it was manufactured to this purpose before , this collector should be checked in two ways the first one is find the collector efficiency by the hot water rotated and the second one check the collector efficiency by produce the steam and the aim of this section is to compare the experimental efficiency with that theoretical as the following:

3.2.1 Hot Water Experimental Efficiency

In this part of the experiment there are many steps it should be done to can get an accurate results before start do the experiment. when connecting the system first of all it need to

calibrate the thermo cables by use a hot water before connected them with the reader device which is connected with computer to record the input and output temperature degrees. in the collector by use memo program, the second step it need to regulated the flow rate inside the system by regulate the water pump speed and throttle the gate valve then check the flow meter indicator to can get the mass flow rate which is rotate inside the system, the other steps it needed to record the ambient temperature degrees by external thermometer and record the solar radiation every time by use the solar radiation device. By measure the flow mass inside the system and the temperature degrees input and output it could calculate the heat gain from the collector by equation no. (2 -15) and the collector experimental efficiency from equation no. (2 -17a) as the following:

- Experiment on 4/12/2018 at 10am

The flow meter measured 2 liters per 4 mints the flow mass it will be

The mass flow rate is $\frac{2}{4 \times 60} = 0.008 \text{ kg/sec.}$, $C_p = 4180 \text{ j/kg.k}$ $T_{in} = 13.7$, $T_{out} = 19.8$

Heat gain by collector

$$Q_{\text{gain}} = \dot{m} c_p (T_{\text{out}} - T_{\text{in}}) \quad (2.15)$$

$$Q_{\text{gain}} = 0.008 \times 4180 \times (19.8 - 13.7)$$

$$Q_{\text{gain}} = 212 \text{ watt/collector}$$

In spite of the collector slope with 15 degree the sun is still with high slope that could not cover the entire pipe receive length in the time of the experiment therefore this case has taken in this calculations by take the actual length of the surface reflected which is measured from the experiment as the following.

Heat gain by m^2 is

$$Q \text{ gain} = \frac{212}{2 \times 1.2}$$

$$Q \text{ gain} = 88 \text{ watt/m}^2$$

The experiment radiation measurement is $G_I = 441 \text{ watt/m}^2$, from excel program the beam transition factor is $\tau_b = 0.615$

The experimental beam radiation is

$$G_b = G_I (1 - \tau_d)$$

The diffuse radiation factor is τ_d

$$\tau_d = 0.271 - 0.294 \tau_b \text{ (1-22 a)}$$

$$\tau_d = 0.09$$

The experimental efficiency is

$$\eta_{exp.} = \frac{m \cdot cp \cdot (T_{out.} - T_{in.})}{A_c \cdot G_b} \quad (2-17a)$$

The experimental beam radiation is

$$G_b = 441 (1 - 0.09)$$

$$G_b = 401 \text{ watt/m}^2.$$

The experimental efficiency is

$$\eta_{ex} = \frac{88}{401}$$

$$\eta_{ex} = 0.22$$

- Experiment on 9/12/2018 at 11:00 am

The flow meter measured 3 liters per 1 mint the flow mass it will be

The mass flow rate is $\frac{3}{60} = 0.05$ kg/sec. , Cp = 4180 j/kg. K.

- At 11:00 am, $T_{in} = 9.4,$ $T_{out} = 10.8$

Heat gain by collector

$$Q \text{ gain} = \dot{m} c_p (T_{out} - T_{in}) \quad (2.15)$$

$$Q \text{ gain} = 0.05 \times 4180 \times (10.8 - 9.4)$$

$$Q \text{ gain} = 292 \text{ watt/ collector}$$

In spite of the collector slope with 15 degree the sun is still with high slope that could not cover the entire pipe receive length in the time of the experiment therefore this case has taken in this calculations by take the actual length of the surface reflected which is measured from the experiment as the following.

Heat gain by m^2 is

$$Q \text{ gain} = \frac{292}{2 \times 1.2}$$

$$Q \text{ gain} = 122 \text{ watt}/m^2$$

The experiment radiation measurement is $G_I = 610$ watt/ m^2 , from excel program the beam transition factor is $\tau_b = 0.63$

The experimental beam radiation is

$$G_b = G_I (1 - \tau_d)$$

The diffuse radiation factor is τ_d

$$\tau_d = 0.271 - 0.294 \tau_b \quad (1-21)$$

$$\tau_d = 0.085$$

The experimental efficiency is

$$\eta_{exp.} = \frac{m \cdot c_p \cdot (T_{out.} - T_{in.})}{A_c \cdot G_b} \quad (2-17a)$$

The experimental beam radiation is

$$G_b = 610 (1 - 0.085)$$

$$G_b = 588 \text{ watt/m}^2.$$

The experimental efficiency is

$$\eta_{ex} = \frac{122}{588}$$

$$\eta_{ex} = 0.21$$

For the same procedures above it could find the experimental efficiency for every hours as the following

- At 12:00 am, $T_{in} = 19.1$, $T_{out} = 20.3$

The mass flow rate is $\frac{3}{60} = 0.05 \text{ kg/sec.}$, $C_p = 4180 \text{ j/kg. K}$

Heat gain by collector

$$Q \text{ gain} = \dot{m} c_p (T_{out} - T_{in}) \quad (2.15)$$

$$Q \text{ gain} = 0.05 \times 4180 \times (20.3 - 19.1)$$

$$Q \text{ gain} = 251 \text{ watt/ collector}$$

By take the actual length of the surface reflected which is measured from the experiment as the following.

Heat gain by m^2 is

$$Q \text{ gain} = \frac{251}{2 \times 1.2}$$

$$Q \text{ gain} = 104 \text{ watt/m}^2,$$

The experiment radiation measurement is $G_I = 580 \text{ watt/m}^2$.

From excel program the beam transition factor is $\tau_b = 0.65$

The experimental beam radiation is

$$G_b = G_I (1 - \tau_d)$$

The diffuse radiation factor is τ_d

$$\tau_d = 0.271 - 0.294 \tau_b \quad (1-21)$$

$$\tau_d = 0.09$$

The experimental efficiency is

$$\eta_{exp.} = \frac{m \cdot cp \cdot (T_{out.} - T_{in.})}{A_c \cdot G_b} \quad (2-17a)$$

The experimental beam radiation is

$$G_b = 580 (1 - 0.085)$$

$$G_b = 530 \text{ watt/m}^2.$$

The experimental efficiency is

$$\eta_{ex} = \frac{104}{530}$$

$$\eta_{ex} = 0.20$$

At 1:00 pm, $T_{in} = 29.8$, $T_{out} = 32$

The mass flow rate is $\frac{3}{60} = 0.05$ kg/sec. , $C_p = 4180$ j/kg. K

Heat gain by collector

$$Q \text{ gain} = \dot{m} c_p (T_{out} - T_{in}) \quad (2.15)$$

$$Q \text{ gain} = 0.05 \times 4180 \times (32 - 29.8)$$

$$Q \text{ gain} = 460 \text{ watt/ collector}$$

By take the actual length of the surface reflected which is measured from the experiment as the following.

Heat gain by m^2 is

$$Q \text{ gain} = \frac{460}{2 \times 1.2}$$

$$Q \text{ gain} = 192 \text{ watt}/m^2,$$

The experiment radiation measurement is $G_I = 735$ watt/ m^2 . From excel program the beam transition factor is $\tau_d = 0.66$

The experimental beam radiation is

$$G_b = G_I (1 - \tau_d)$$

The diffuse radiation factor is τ_d

$$\tau_d = 0.271 - 0.294 \tau_b \quad (1-21)$$

$$\tau_d = 0.077$$

The experimental efficiency is

$$\eta_{exp.} = \frac{m \cdot c_p \cdot (T_{out.} - T_{in.})}{A_c \cdot G_b} \quad (2-17a)$$

The experimental beam radiation is

$$G_b = 735 (1 - 0.077)$$

$$G_b = 678 \text{ watt/m}^2.$$

The experimental efficiency is

$$\eta_{ex} = \frac{192}{678}$$

$$\eta_{ex} = 0.28$$

At 2:00 pm, $T_{in} = 38$, $T_{out} = 42$

The mass flow rate is $\frac{3}{60} = 0.05 \text{ kg/sec.}$, $C_p = 4180 \text{ j/kg. K}$

Heat gain by collector

$$Q \text{ gain} = \dot{m} c_p (T_{out} - T_{in}) \quad (2.15)$$

$$Q \text{ gain} = 0.05 \times 4180 \times (42 - 38)$$

$$Q \text{ gain} = 836 \text{ watt/ collector}$$

By take the actual length of the surface reflected which is measured from the experiment as the following.

Heat gain by m^2 is

$$Q \text{ gain} = \frac{836}{2 \times 1.2}$$

$$Q \text{ gain} = 348 \text{ watt/m}^2,$$

The experiment radiation measurement is $G_I = 670 \text{ watt/m}^2$. From excel program the beam transition factor is $\tau_b = 0.64$

The experimental beam radiation is

$$G_b = G_I (1 - \tau_d)$$

The diffuse radiation factor is τ_d

$$\tau_d = 0.271 - 0.294 \tau_b \quad (1-21)$$

$$\tau_d = 0.082$$

The experimental efficiency is

$$\eta_{exp.} = \frac{m \cdot cp \cdot (T_{out.} - T_{in.})}{A_c \cdot G_b} \quad (2-21a)$$

The experimental beam radiation is

$$G_b = 670 (1 - 0.082)$$

$$G_b = 615 \text{ watt/m}^2.$$

The experimental efficiency is

$$\eta_{ex} = \frac{348}{615}$$

$$\eta_{ex} = 0.57$$

At 3:00 pm, $T_{in} = 46.1,$ $T_{out} = 49$

The mass flow rate is $\frac{3}{60} = 0.05 \text{ kg/sec.}$, $C_p = 4180 \text{ j/kg. K}$

Heat gain by collector

$$Q \text{ gain} = \dot{m}cp (T_{out} - T_{in}) \quad (2.19)$$

$$Q \text{ gain} = 0.05 \times 4180 \times (49 - 46.1)$$

$$Q \text{ gain} = 606 \text{ watt/ collector}$$

By take the actual length of the surface reflected which is measured from the experiment as the following.

Heat gain by m^2 is

$$Q \text{ gain} = \frac{606}{2 \times 1.2}$$

$$Q \text{ gain} = 252 \text{ watt}/m^2,$$

The experiment radiation measurement is $G_I = 580 \text{ watt}/m^2$. From excel program the beam transition factor is $\tau_b = 0.64$

The experimental beam radiation is

$$G_b = G_I (1 - \tau_d)$$

The diffuse radiation factor is τ_d

$$\tau_d = 0.271 - 0.294 \tau_d \quad (1-21)$$

$$\tau_d = 0.082$$

The experimental efficiency is

$$\eta_{exp.} = \frac{m \cdot cp \cdot (T_{out.} - T_{in.})}{A_c \cdot G_b} \quad (2-21a)$$

The experimental beam radiation is

$$G_b = 580 (1 - 0.082)$$

$$G_b = 532 \text{ watt}/m^2.$$

The experimental efficiency is

$$\eta_{ex} = \frac{252}{532}$$

$$\eta_{ex} = 0.47$$

At 4:00 pm, $T_{in} = 38.7$, $T_{out} = 40.3$

The mass flow rate is $\frac{3}{60} = 0.05$ kg/sec. , $C_p = 4180$ j/kg. K

Heat gain by collector

$$Q \text{ gain} = \dot{m}c_p (T_{out} - T_{in}) \quad (2.15)$$

$$Q \text{ gain} = 0.05 \times 4180 \times (40.3 - 38.7)$$

$$Q \text{ gain} = 334 \text{ watt/ collector}$$

By take the actual length of the surface reflected which is measured from the experiment as the following.

Heat gain by m^2 is

$$Q \text{ gain} = \frac{334}{2 \times 1.2}$$

$$Q \text{ gain} = 139 \text{ watt}/m^2,$$

The experiment radiation measurement is $G_I = 345$ watt/ m^2 . From excel program the beam transition factor is $\tau_b = 0.53$

The experimental beam radiation is

$$G_b = G_I (1 - \tau_d)$$

The diffuse radiation factor is τ_d

$$\tau_d = 0.271 - 0.294 \tau_b \quad (1-21)$$

$$\tau_d = 0.12$$

The experimental efficiency is

$$\eta_{exp.} = \frac{m \cdot cp \cdot (T_{out.} - T_{in.})}{A_c \cdot G_b} \quad (2-21a)$$

The experimental beam radiation is

$$G_b = 345 (1 - 0.12)$$

$$G_b = 303 \text{ watt/m}^2.$$

The experimental efficiency is

$$\eta_{ex} = \frac{139}{303}$$

$$\eta_{ex} = 0.46$$

The table 3-1 show the experimental data for hot water from the from the previous calculations

Table 3-1 Experimental data table for heat water

Date	Time	Flow rate kg/sec.	Inlet temp.	Outlet temp.	Beam transition factor	Diffuse transition factor	instrument radiation watt/m²	Exp. Beam radiation Watt/m²	Heat gain Watt/m²	Efficiency
09/12/2018	11:00 AM	0.05	9.4	10.8	0.63	0.085	610	558	122	0.22
09/12/2018	12:00pm	0.05	19.1	20.3	0.65	0.09	580	528	104	0.19
09/12/2018	13:00pm	0.05	29.8	32	0.66	0.077	735	676	192	0.23
09/12/2018	14:00:pm	0.05	38	42	0.64	0.082	670	616	348	0.57
09/12/2018	1500:pm	0.05	46.1	49	0.64	0.082	580	533	252	0.47
09/12/2018	16:00pm	0.05	38.7	40.3	0.53	0.12	345	303	139	0.46
04/12/2018	11:00 AM	0.008	13.7	19.8	0.615	0.09	441	401	88	0.22



Figure 3. 10 Shows the heat gain theoretically & experimentally in the day.

The figure (3-10) above shows the heat gain daily shine hours and it could observe that the heat gain theoretically is too higher than the experimental heat gain at the beginning because our experiment done in the cold weather and the system was started from freezing and sometimes weather be cloudy then it increase dramatically when system get the steady state at 2:00 while the theoretical heat gain shows that heat gain starts increase in the morning hours and get the maximum at afternoon then decrease again.

Figure 3. 11 Shows the collector efficiency theoretically & experimentally in the day

The figure (3-11) shows that theoretical efficiency is constant on (0.63) because there is no change in percentage of the heat useful and then beam radiation theoretically and the heat losses in surfaces reflector and absorber it consider constant theoretically while the experimental efficiency it start very low and increase to be near the theoretically at 2:00 pm because the system it start from freezing point in the morning then heated and increase its efficiency dramatically. From this chart it could note the difference between the theoretical and experimental efficiency and that because numbers of the following

- There is difference between the weather clearness because it could be some times cloudy or moisture in the weather or there is some dust make the solar radiation less than theoretically calculation.
- The collector surface may be not clean completely or face to face with sun directly all the time. May be there is some deviation in the collector direction make the solar radiation reflected to the absorber less than the theoretically.
- There is some tolerance in some suppose properties like the size and dimensions of the tube and some tolerance in the instruments calibration like the solar radiation device and thermo cables calibration and flow meter measurement.

All these properties could be stand behind the difference between the theoretical and experimental and values.

3.2.2 Steam Experimental Efficiency

In this part of the section it should check the actual mass steam which it could get by the collector and compare it with mass steam which it could get it theatrically to find the collector efficiency to produce the steam.

- Experiment on 20/11/2018 at (1:00 - 2:00) pm

In this experiment the receiver tube split of the system by the gate valve before and after the receiver tube then the water trapped in the tube the mass flow inside the tube measure by filling the tube and drainage the water inside by indictor measuring drum then close the gate valves and check the water remain in the tube after evaporated to measure the steam produce by the collector as the following

The tube volume = 3.2 litter

The water remain in the tube after evaporate = 1.75 liter

Actual Steam produce = 3.214 -1.75

Actual Steam produce = 1.464 liter (for the collector.)

By take the actual length of the surface reflected (1.2) m it could find

$$\text{Actual Steam produce}/m^2 = \frac{1.464}{2 \times 1.2}$$

$$\text{Actual Steam produce}/m^2 = 0.61 \text{ kg}/m^2\text{hr.}$$

The total radiation experimentally $G_I = 668 \text{ watt}/m^2$

Beam transition factor

$$\tau_b = 0.66$$

The beam radiation experimental

$$G_b = G_I (1 - \tau_d)$$

The diffuse radiation factor τ_d

$$\tau_d = 0.271 - 0.294 \tau_b \quad (1-21)$$

$$\tau_d = 0.077$$

The beam radiation experimentally

$$G_b = 668 \times (1 - 0.077)$$

$$G_b = 616$$

$$G_b = 616 \text{ kw/m}^2$$

From the vapor tables at pressure 0.1 Map, $h_{fg} = 2258 \text{ kj/kg}$,

The heat useful gain theoretically from excel program is 460watt.

$$\text{Steam produce theoretically} = \frac{426 \times 3.6}{2258}$$

$$Q_{\text{steam generate th.}} = 0.68 \text{ kg/m}^2\text{hr}$$

The experimental efficiency is

$$\eta_{exp.} = \frac{m \cdot h_{fg}}{G_b \cdot 3.6}$$

$$\eta_{exp.} = \frac{0.61 \times 2258}{616 \times 3.6}$$

$$\eta (\text{exp.}) = 0.62$$

The theoretical efficiency is

$$\eta_{th.} = \frac{0.68 \times 2258}{673 \times 3.6}$$

$$\eta_{th.} = 0.63$$

Table 3. 2 Experimental data table for steam

Date	Time radiation	Beam transition factor	Diffuse transition factor	Measurement radiation Watt/m²
20/11/2018	1:00- 2:00 pm	0.66	0.077	668

Experimental. Beam radiation Watt/m²	Steam generates theoretically Kg/m².hr.	Steam generate experimentally. Kg/m².hr.	Theoretical efficiency	Experimental efficiency
616	0.68	0.61	0.63	0.62

CHAPTER 4

CONCLUSIONS AND RECOMMENDATIONS

4.1 Conclusion

This chapter is the last station in this research through in it could estimate the performance of the parabolic trough collector technology to produce the heat water and steam from both theoretical and practical aspect of this study. Depend on that it could say it is suitable way to produce the heat water and generated steam with electrical produce station and industrial project until in the low radiation areas by develop some technique to make it suitable in these areas.

However, there are some problems it could face this technology in some regions like Kayseri. instead of solve the problem of the sun set which make the solar source is not continue per a day by use the storage tank with molten salt and other artificial material there is another problem which is the cloudy and freezing weather in winter season that make the sun source energy very low and it is impossible depend on it only in this period.

The other problem which it has faced in the experiment is the sun radiation deviation of the collector at the hourly day because of the different in the sun altitude angles (α) that make the radiation couldn't cover the entire collector and let a part of the collector outside the work in spite of the collector sloped by 15 degree.

From the experimental part of this study it could note there is a great advantage by use the tilted collector to get the highest solar radiation level by increase the slope of the

collector according to solar altitude angles which was calculated in the last part of excel program as illustrated in chapter 2.

4.2 Recommendations

Refer to the motioned above it needs to use the following recommendations:

- To overcome of the cloudy and freezing problem in the winter season in some regions which face this case it need to use the hybrid stations with fuel source to offset the shortage in solar energy in this period.
- To can solve the experimental problem of solar radiation deviation which makes the radiation couldn't cover the entire collector receiver in the researches experiments. It could recommend using flexible collectors that could change its slope angle to matching the solar altitude angles.
- According to the maximum useful from solar radiation that could get from tilted collector. it could recommended to increasing the researches which study in how to create a new generation of parabolic trough in solar electrical power stations that able to use a collectors with a flexible change slope angles it make the collector follow and face the sun in both directions instead of the one direction as it is used in the modern electrical stations. (Like the mirror fields in solar tower technology). In the designed collector, the direct solar radiation measured on November 20 was 0.61 kg / h steam at 616 W / m². The amount could make by two-axis collector's solar tracking system is 1.107 Kg / h steam can be obtained.

In spite of the difficulties and perhaps the increasing cost of the new design, the high radiation that could get by the new design may be make it more successful and suitable for a large range of areas which have a low solar radiation.

This technology could be used to heating houses also. For example the house which has 180 m² and heat loses 17.55 kW for November in Kayseri it needs nearly 7 collectors in the same specific design of our experimental collector and it be enough to heating the house so the estimating cost for a system like this with all parts (collector with vacuumed tube, piping & insulation system, carrier, water pump) it is nearly 7000 \$ for a house.

REFERENCES

1. Cumpston, J., Mitsos, A., 2017. Concentrating solar Thermal overview The Globe Home of Chemical Engineering Concentrated Solar Thermal Overview **CEP Magazine Aiche**. 1-10.
2. Tzivanidis, C., Bellos, E., Korres, D., Antonopoulos, K.A., 2015. Mitsopoulos G. 2015. Thermal and Optical Efficiency Investigation of a Parabolic Trough Collector. **Case Studies in Thermal Engineering**, Vol. 6, pp. 226-237.
3. Rolim, M., Fraidenraich, N., 2009. Analytic modeling of a solar power plant with parabolic linear collectors. **Solar Energy** Vol. 83, pp. 126-133.
4. Fernández, A., Zarzaa, E., 2010. Parabolic-trough solar collectors and their applications. **Renewable and Sustainable Energy Reviews**, Vol. 14, pp. 1695-1721.
5. Liu, Q., Yang, M., 2012. Modeling and optimizing parabolic trough solar collector systems using the least squares support vector machine method. **Solar Energy**, Vol. 86, pp. 1973-1980.
6. Zhifen, L., Yuang, G., 2013. Dynamic test model for the transient thermal performance of parabolic trough solar collectors. **Solar Energy**, Vol. 95 pp. 65-78.
7. Reddy, K.S., Kumar, K., 2015. Experimental investigation of porous disc enhanced receiver for solar parabolic trough collector. **Renewable Energy**, Vol. 77, pp. 308-319.
8. Jebasingh, V.K., Joselin, G.M., 2016. A review of solar parabolic trough collector. **Renewable and Sustainable Energy Reviews**, Vol. 54, pp. 1085-1091.
9. Wanjun, Q., Wang, R., 2017. Test of a solar parabolic trough collector with rotatable axis tracking. **Applied Energy**, Vol. 207, pp.7-17.
10. Hoseinzadeha, H., Kasaeian, A., 2018. Geometric optimization of parabolic trough solar collector based on the local concentration ratio using the Monte Carlo method. **Energy Conversion and Management**, Vol 175, pp. 278-287.
11. Haojie, X., Yinshi, L., 2019. Transient model and characteristics of parabolic-trough solar collectors: Molten salt vs. synthetic oil. **Solar Energy**, Vol. 182, pp. 182-193.
12. Hafez, A.Z., Attia, A.M., 2018. Design analysis of solar parabolic trough thermal collectors. **Renewable and Sustainable Energy Reviews**, Vol. 82, pp. 1215-1260.

13. Matteo, B., Simone, D., 2016. Experimental study of a parabolic trough solar collector with flat bar-and-plate absorber during direct steam generation. **Energy**, vol. 116, pp. 1039-1050.
14. Karima, G., Safa, S., 2019. Thermal analysis of linear solar concentrator for indirect steam generation. **Energy Procedia**, Vol. 162, pp. 136-145.
15. Wald, L., 2009. Solar Energy Conversion and Photoenergy Systems. **Solar radiation energy (fundamentals) vol-1**. Solar energy conversion and photo energy systems, Paris, France.371.
16. John, A., William, A., **Solar Engineering Of Thermal Processes Gear Team Fourth Edition**. New Jersey in Canada.910.
17. Greif, J., Scharmer, K., 2000.**The European Solar Radiation Atlas vol. 1: Fundamentals and Maps**. Paris. 98.
18. Günther, M., 2010.**Enernena Advanced CSP Teaching Materials chapter 2: Solar Radiation**. Germany. 88.
19. Hizam, H., Gomes, C., 2017. Estimation of Hourly, Daily and Monthly Global Solar Radiation on Inclined Surfaces: Models Re-Visited. **Energies**.
20. David, P., 2004. **Latitude and Longitude**. (http://www.nasa.gov/about/highlights/hp_privacy.htm/).9-7-2014.
21. Montgomery, M., Malloy, N., **Introduction to Coordinate Systems / Spatial Reference Systems**. (http://gsp.humboldt.edu/olm/Lessons/GIS/01%20SphericalCoordinates/Latitude_and_Longitude.html).2018.
22. Wald, L., 2018. Basics in solar radiation at earth surface. **Hal Arcgives-Ouvertes**.
23. Crespo, L., Dobrotkova, Z., Philibert, C., 2012. Concentrating Solar Power. **Renewable Energy Technologies: Cost Analysis Series Volume 1**. International Renewable Energy Agency. Germany.
24. Cardozo, F.R., 2012. Concentrating solar Power Technologies Using Molten Salts for Storage and Production of Energy. **Master's Degree Thesis** pp. 1-86.
25. Philibert, C., Frankl, P., 2010. Concentrating Solar Power. **Technology Roadmap**. iea international energy agency pp.1-45.
26. Bernhard, R., Lalaing, J., 2008. Linear Fresnel Collector Demonstration on the Psa- Part I – Design; Construction and Quality Control. **Research Gate** pp. 1-10.
27. Barlev, D., Vidu, R., 2011. Solar Energy Materials & Solar Cells. **Elsevier** pp. 2703–2725.

28. Geok, L., Ruddin, M., 2014. A Review of Parabolic Dish-Stirling Engine System Based on Concentrating Solar Power. **Telkonnika** Vol.12 pp. 1142~1152.
29. Bettzüge, M., Amin, A., 2011. Concentrating solar power: it's potential Contribution to a Sustainable Energy Future. **European Academics Science Advisory Council**. pp. 1-57.
30. Inamita, p., Kadam, V., 2013. Concentrating Solar Power (Csp) Systems. **International Journal of Electrical, Electronics and Data Communication**. PP. 2320-2084.
31. Günther, M., Joemann, M., Csambor, S., 2010. **Enermena Advanced CSP Teaching Materials chapter 5: Parabolic Trough Technology**. Germany.106.
32. Mahinder, B., Sulaiman, F., 2003. Designing a Solar Thermal Cylindrical Parabolic Trough Concentrator by Simulation. **International Rio3 Congress, world climate and energy event**. pp. 1-6.
33. Rajan, A., Hemanth, S., 2014. Reduction of Heat Losses in Parabolic Trough Collector Using Vacuum Seal. **Ird India** PP. 2321-5747.
34. Nowak, H., 1988. **The Sky Temperature in Net Radiant Heat Losses Calculations From Low- Sloped Roofs**. Great Britain 232.
35. Sintali,I., Egbo, G., Dandakouta, H., 2014. Energy Equations for Computation of Parabolic-Trough Collector Efficiency Using Solar Position Coordinates. **American Journal of Engineering Research (AJER)** pp.25-33.
36. Patana, N., 2013. Improvements in efficiency of solar parabolic trough. **Iosr Journal of Mechanical and Civil Engineering (IOSR-JMCE)**. PP 63-75.
37. Abdullah, A., AlZahrana, B., Dince, I., 2018. Energy Conversion and Management. **ALSEVIER** PP 476-488.
38. Malvi1, C., Gupta, A., 2017. Experimental investigation of heat removal factor in solar flat plate Collector for various flow configurations. **International Journal of Green Energy** pp. 442-448.
39. Mishra, R.S., 2018. Performance analysis of solar parabolic trough collectors driven combined supercritical CO₂ and organic Rankine cycle. **Engineering Science Technology, an International Journal** pp. 451-464.
40. David, H., Sophie, V., 2006. A Linear Parabolic Trough Solar Collector Performance Model. **Proceedings of the Sixth International Conference for Enhanced Building Operations, Shenzhen, China, November 6 - 9, 2006**.

41. Struckmann, F., 2008. Analysis of a Flat-plate Solar Collector. **Project Report 2008 MVK160 Heat and Mass Transport**. May 08, 2008, Lund, Sweden.
42. Amit, K., Nitesh, K., Shailendra, N., 2018. Performance Study of a Cylindrical Parabolic Concentrating Solar Water Heater with Nail Type Twisted Tape Inserts in the Copper Absorber Tube. **Energies** PP 1-15.
43. Cocci, G., 2016. Parabolic Trough Collector Prototypes for Low-Temperature Process Heat. **Springer Briefs in Applied Sciences and Technology**. PP 13-39.



CURRICULUM VITAE

Name : Ammar Sabah Ahmed AL-Amili
 Nationality : Iraqi
 Date of Birth : 30 -3 – 1976
 Marital Status : Married.
 Contact : 0096407902424914 (Iraq) (whatsapp), 00905379947925 (turkey).
 E-mail : amaralamili@yahoo.com

EDUCATION

1994-1999:

Bachelor of Science in MECHANICAL ENGINEERING (B.SC.)

College Of Engineering, Al- Mustansiria University Baghdad- Iraq.

PROFESSIONAL EXPERIENCE

Piping engineer with 15 years a practical experience of (design, implementation,) in industrial field.

(3/2/2017- 15/1/ 2019)

Study Msc. program with thesis (English) for department of mechanical engineering in (ERCIYES University) in turkey.

(8/9 /2016- 21/1/ 2017)

First Semester for the master degree (CANKAYA University) in Turkey.

(Feb. /2015- may/ 2016)

State Design and implement projects Company. (Sector Comp.)

Position: Site Manager.

Project involved:

- Execute (75m³/h) Industrial West Water Treatments (chemical& biology) for edible oil factory at (Mesan city).

Responsibilities: manage the site staff (civil, mechanical, electrical) engineers and technical to execute the project.

(Fib /2014- Jan/ 2015)

State Design and implement projects Company. (Sector Comp.)

Position: Site Engineer.

Project involved: Execute (6) Storage Tank Stainless Steel (650) m³ for edible oil in three sites in (Baghdad).

Responsibilities: Fabricate, Install, Welding the stainless steel plates of the tanks.

(Desm /2012- Jan. 2014)

State Design and implement projects Company. (Sector Comp.)

Position: Site Engineer.

Project involved:

- Execute (75 m³/h) Industrial West Water Treatments (chemical) for edible oil factory at Baghdad.

Responsibilities: execute the piping network and install the equipment.

(mar.2012 – NOV.2012)

AL-ANI Comp. for Contracts work as a subcontractor with FLUOR Comp. (Private Comp.)

Position: Piping Site Engineer.

Project involved: execute the Metering Skids piping network for three digasofire stations (6-7-8 units) at West al- Qurnaa.

Responsibilities: execute the piping net, shoes, and supports at fabricate Shop & install it at the site.

(Jan. /2011- Apr. /2012)

Al-mustansiriya university engineering consultation bureau. (Private Work).

Position: Design Engineer.

Project involved: design basic & details drawings for the following projects:

- Piping System of steam & condensate, for Oil Storage Tanks at al- Najaf with ministry of oil.
- Piping system of steam & condensate, heavy & light network piping fuel for al Najaf electrical Power Station.
- Fire Fighting Piping network system for oil product distribution comp. building with ministry of oil at al –Dora refinery.
- Air condition system for drags storage building at Baghdad.
- Air condition system for ministry of communication internet building at Baghdad.

(DEC. 2009 -OCT. 2010)

AL NUKHBA Company for contractor work as subcontractor with PROKOP comp. (Private Comp.)

Position: Piping Site Engineer.

Project involved: execute the network piping for (70,000 Bl/day) Oil Refinery at (Al-Doura refinery) in (Baghdad).

Responsibilities: execute the piping network.

(Nov. 2008-OCT. 2009)

CAR Comp. for contractor work as subcontractor with DANA GAS comp. (Private comp.)

Position: Supervisor piping network & field Engineer.

Project involved: Execute Natural Gas (Kho more) Refinery at (Al-Lusitania city) & 10000 Br/day for two units Oil Refinery at (Erbil city).

Responsibilities: Check the p&id and isometric drawings with the implement of the network piping in the site.

(Oct. 2005-jul. 2008)

International Free Company Ltd. For Contracts. (Private comp.)

Position: Piping Design & Supervisor Engineer.

Project involved: Design the layout plan, general arrangement plots, isometric sketch,

nozzle orientation, pressure vessel data sheets & Bill of material with specification for Electrical gas turbine station (16 x 25 Mwat.) Unites in Al-zufrania power plant in (Baghdad).

Responsibilities:

- Design & supervisor of construction Piping & layout network for (light & heavy fuel oil and all other utility like steam, condensate, water, compress air...)
- Supervisor of construction Six storage tanks (5000 m3) (23000 diam.) for fuel and water & pressure vessels.
- Design & make data sheet for pressure vessels.
- Design & supervisor of construction Piping & layout network to the water treatment (clarify water, R.O. water & softener water units)
- Layout & Install all equipment like (emergency generator boilers, heavy fuel treatment, heavy fuel heaters and all other auxiliary equipment with turbine.

(mar. 2005- Oct. 2005)

Euro projects International ltd.Fze. For Trading. (Private Comp.)

Position: Sale Engineer & Technical Support.

Project involved: send & receive the commercial letters between (Baghdad &Dubai), make the commercial & technical offers in (Baghdad office).

Responsibility:

- Send & receive the commercial letter.
- Make the commercial, technical & cover letters.
- Check the specifications required with the tender.
- Follow up the contracts.

(Des.2002-mar.2005)

Industrial Design and Consultation State Company. (Sector Comp.)

Position: Site Engineer

Project involved: Engineer in charge of the following projects:

1. Execute a potable water network (ductile iron pipe).
2. Execute the project of install 2 large boilers (water tube type) with (75 m3/hr.) make the pipe connection between the drums & pipe fire walls.
3. Execute the steam & water service network system distributed from boiler station (5

boilers) at the state company for the dairy products.

4. Make drawings as built the piping system and layout to nine substations pumping of the Human water treatment station in al Rustumia Station.

Responsibilities:

- Follow up Authorities approvals, Prepare construction plan.
- Prepares equipment and material which it needs in the Construction.
- Take all necessary measures required on the site before construction to avoid make the mistakes with approval planning.
- Gives the instructions of the suitable construction method.

OCT.2000-DES.2002

State Industrial Design and Consultation Company. (Sector Comp.)

Position: Designer piping Engineer.

Project involved Design plots for the following projects (newspaper ink factory, carbonate al sodium project, methanol plant).

Responsibilities:

- Design layout project equipment with coordinate axes.
- Design the general arrangement piping connection depend on the P& Id. by Divided the all area of plot plan with coordinate to show all details of these areas.
- Make nozzle orientation to equipment and vessels in the project.
- Make isometric sketch to pipe lines with all instruments on it.
- Make the bills of material with specification to all pipes with valves, fitting, flanges,)
- Design the trenches and pipe rack of project.

COMPUTER SKILLS

- 3D-Max. Design all the area of project with equipment and piping net with scale by (3D –MAX) Program.
- Auto CAD (2-dimintion, isometric).
- Microsoft office (word and excel).

ADDITIONAL QUALIFICATION AND MEMBERSHIP

Member of Iraqi Engineers Union.

LANGUAGE: English and Arabic fluently.

